



## Research paper

# miR-424 coordinates multilayered regulation of cell cycle progression to promote esophageal squamous cell carcinoma cell proliferation



Jing Wen<sup>a,b,1</sup>, Yi Hu<sup>b,c,1</sup>, Qianwen Liu<sup>b,c,1</sup>, Yihong Ling<sup>d</sup>, Shuishen Zhang<sup>e</sup>, Kongjia Luo<sup>b,c</sup>, Xiuying Xie<sup>a,b</sup>, Jianhua Fu<sup>a,b,c,2</sup>, Hong Yang<sup>a,b,c,\*</sup>

<sup>a</sup> State Key Laboratory of Oncology in South China, Collaborative Innovation Center for Cancer Medicine, Sun Yat-sen University Cancer Center, 651 Dongfeng East Road, Guangzhou 510060, China

<sup>b</sup> Guangdong Esophageal Cancer Institute, 651 Dongfeng East Road, Guangzhou 510060, China

<sup>c</sup> Department of Thoracic Oncology, Sun Yat-sen University Cancer Center, 651 Dongfeng East Road, Guangzhou 510060, China

<sup>d</sup> Department of Pathology, Sun Yat-sen University Cancer Center, 651 Dongfeng East Road, Guangzhou 510060, China

<sup>e</sup> Department of Thoracic Surgery, The First Affiliated Hospital of Sun Yat-sen University, 58 Zhongshan Second Road, Guangzhou 510080, China

## ARTICLE INFO

## Article history:

Received 2 August 2018

Received in revised form 15 October 2018

Accepted 15 October 2018

Available online 23 October 2018

## Keywords:

miR-424

Esophageal squamous cell carcinoma

Cell cycle

Cell proliferation

## ABSTRACT

**Background:** Dysregulation of the cell cycle has been implicated in esophageal squamous cell carcinoma (ESCC) progression. This study aimed to evaluate the role of miR-424 in cell cycle regulation and ESCC proliferation.

**Methods:** The role of miR-424 in cell proliferation was evaluated *in vitro* and *in vivo*. Transcriptional activation of miR-424 was determined using chromatin immunoprecipitation, and binding of miR-424 to targets was verified using miRNA ribonucleoprotein complex immunoprecipitation.

**Findings:** miR-424 was upregulated and correlated with poor survival in ESCC patients. Repression or overexpression of miR-424 respectively decreased or increased ESCC cell proliferation *in vitro* and *in vivo*. miR-424 expression is transcriptionally regulated by E2F1 and increased during G1/S transition. Knockdown or overexpression of miR-424 respectively inhibited or promoted both G1/S and G2/M cell cycle transitions in ESCC cells, and these effects were mediated by two newly identified miR-424 targets, PRKCD and WEE1, respectively. Consequently, elevation of PRKCD by miR-424 knockdown led to enhanced stability of the p21<sup>Cip1</sup> protein via increased activation of PRKCD and downstream p38 MAPK and JNK signaling to block CDK2 activation and G1/S transition, while elevated WEE1 maintained CDC2 in an inactive state to block G2/M transition. However, circLARP4 could sponge the binding of miR-424 to PRKCD, thus compromising the regulation of G1/S progression by miR-424.

**Interpretation:** miR-424 coordinates a previously unknown, multilayered regulation of ESCC cell cycle progression to promote ESCC proliferation, and may be used as a novel prognostic marker and an effective therapeutic target for ESCCs.

**Fund:** National Natural Science Foundation of China.

© 2018 The Authors. Published by Elsevier B.V. This is an open access article under the CC BY-NC-ND license (<http://creativecommons.org/licenses/by-nc-nd/4.0/>).

## 1. Introduction

Esophageal cancer is one of the most aggressive malignancies of the gastrointestinal tract. Esophageal squamous cell carcinoma (ESCC) is the globally predominant pathological type of esophageal cancer [1]. In China, ESCC, which accounts for most malignant esophageal tumors, ranks as the third most common malignancy and the fourth most common cause of cancer-related death [2]. The risk factors for ESCC are thought to be related to dietary and lifestyle habits, as well as genetic polymorphisms [3]. However, the complicated molecular mechanisms

underlying ESCC development and progression are not yet fully understood.

The cell cycle, the process by which cell division occurs, is a series of highly regulated steps that are orchestrated at the molecular level by the sequential activation or inactivation of cyclin-dependent kinases (CDKs); the activities of CDKs depend upon physical interactions with positive regulatory subunits cyclins or negative regulatory subunits known as CDK-inhibitory proteins (CKIs) [4]. Impaired function of critical gatekeepers of cell cycle progression caused by the accumulation of alterations involving the cell-cycle regulatory machinery will allow unscheduled persistent cell proliferation, which is a hallmark of cancer [5]. Dysregulation of the cell cycle by genomic perturbations, genetic mutations, and (or) altered expression of key molecules has been implicated in ESCC development [3,6].

\* Corresponding author at: 651 Dongfeng East Road, Guangzhou 510060, China.

E-mail address: [yanghong\\_cn@outlook.com](mailto:yanghong_cn@outlook.com) (H. Yang).

<sup>1</sup> Authors contributed equally.

<sup>2</sup> Senior authors contributed equally.

## Research in context

### Evidence before this study

*miR-424* was previously reported to exert a primarily tumor suppressive role in most types of cancers, such as breast cancer, cervical cancer, hepatocellular carcinoma, colon cancer, and leukemia. However, our preliminary microarray studies identified *miR-424* as one of the most significantly upregulated miRNAs in esophageal squamous cell carcinoma (ESCC) tissues compared with normal esophageal tissues, suggesting a tumor-promoting role of it in ESCCs.

### Added value of this study

Here, we proved that *miR-424* is upregulated in ESCC and correlates with poor survival among ESCC patients. The expression of *miR-424* is elevated along with cell cycle progression from G0/G1 to S-phase, which is transcriptionally regulated by G1/S transcription factor E2F1. In ESCCs, *miR-424* exerts its tumor-promoting role by cell-cycle-phase specifically targeting *PRKCD* and *WEE1*, which induces subsequent changes in the expression levels or activities of downstream cyclin-dependent kinases (CDKs) or CDK inhibitory proteins (CKIs), to regulate G1/S and G2/M cell cycle transition, respectively. Furthermore, *circLARP4*, a natural sponge of *miR-424* during G1/S transition, decreases *miR-424* binding to *PRKCD* and modulates the effect of *miR-424* on G1/S transition.

### Implications of all the available evidence

Our study highlights an important tumor-promoting role for *miR-424* in regulating ESCC cell cycle progression; *miR-424* may possibly be used as a novel prognostic marker and an effective therapeutic target for ESCCs.

MicroRNAs (miRNAs) are single-stranded non-coding small RNA segments that operate *via* sequence-specific interactions with the 3' untranslated regions (3'UTRs) of mRNA targets to suppress translation and mRNA decay to regulate gene expression post-transcriptionally [7]. These molecules have been reported to be dysregulated in virtually all human cancer types, including ESCC, and function as either tumor suppressors or oncogenes [8]. To identify miRNAs that are potentially involved in ESCC development, we evaluated the miRNA profiles of ESCC and esophageal normal epithelia (NEs) tissues and identified *miR-424* as one of the most significantly upregulated miRNAs in ESCC tissues compared with NE tissues, suggesting a tumor-promoting role of *miR-424* in ESCCs. A role of *miR-424* in inhibiting epithelial-mesenchymal transition and decreasing invasion and migration of ESCC cells has been previously shown [9]. Moreover, *miR-424* exerts a primarily tumor-suppressing role in most types of cancers, such as breast cancer [10], cervical cancer [11,12], hepatocellular carcinoma [13], and leukemia [14]. *miR-424* has also been demonstrated to target the cell cycle regulators *cyclin E1*, *cyclin D1* [15], *CHK1* [12] and *CDC25A* [16] to impair G1/S or G2/M cell cycle transition and delay cell proliferation.

The specific role of *miR-424* in ESCC proliferation and the underlying mechanisms remain unknown. In this study, we characterized the tumor-promoting role of *miR-424* in ESCC proliferation. Further in-depth studies led to the identification of previously unrecognized transcriptional regulators of *miR-424* expression and the elucidation of the direct targets and capacities of *miR-424* in coordinating ESCC cell cycle progression.

## 2. Materials and methods

### 2.1. Clinical specimens

This study was approved by the Research Ethics Committee of Sun Yat-sen University Cancer Center. The 30 ESCC samples and ten NE samples used for miRNA profiling analysis were collected as described in our previous studies [17,18]. Freshly frozen tissues from 60 paired NE and ESCC tissues and 190 ESCC tissues used for quantitative real-time polymerase chain reaction (qRT-PCR) analysis of *miR-424* expression were obtained from ESCC patients undergoing complete surgical esophagectomy with no neoadjuvant or adjuvant treatment from March 2002 to October 2008 in the Department of Thoracic Oncology. The fresh tumor samples were taken from macroscopically judged neoplastic regions, and NE samples were from macroscopically judged normal regions at the surgical resection margin at least 3 cm distant from tumor regions. For each sample, an adjacent tissue sample was stained with hematoxylin and eosin and assessed for the presence or absence of ESCC or NE cells by pathologists. In addition, 110 formalin-fixed and paraffin-embedded (FFPE) ESCC tissue and 60 paired NE tissue samples that were randomly selected from these above 190 ESCC cases were used for immunohistochemistry (IHC) analyses of *PRKCD* and *WEE1* protein expression. Tumor stage was evaluated according to the seventh edition of the American Joint Committee on Cancer tumor-node-metastasis (TNM) staging system.

### 2.2. Reagents and antibodies

Puromycin (Cat# P9620), thymidine (Cat# T18S95), nocodazole (Cat# M1404), propidium iodide (Cat# P4170), cycloheximide (Cat# C7698), and crystal violet (Cat# C6158) were purchased from Sigma-Aldrich Corporation (St. Louis, MO, USA). Rabbit anti-pHH3 (Ser10, Cat# 3377) and a goat anti-rabbit IgG secondary antibody conjugated with Alexa Fluor 647 (Cat# A-21244) used for flow cytometry were purchased from Cell Signaling Technology (Danvers, MA, USA) and Life Technologies/Thermo Fisher Scientific Technology (Carlsbad, CA, USA), respectively.

For western blotting, the primary antibodies anti-*PRKCD* (Cat# 9616), anti-p-*PRKCD* (Thr505, Cat# 9374), anti-*WEE1* (Cat# 4936), anti-p21<sup>Cip1</sup> (Cat# 2947), anti-p27<sup>Kip1</sup> (3686), anti-p-*CDK2* (Thr160, Cat# 2561), anti-*CDK2* (Cat# 2546), anti-p-*CDC2* (Tyr15, Cat# 4539), anti-*LATS2* (Cat# 13646), anti-*PDCD4* (Cat# 9535), anti-*CDC25A* (Cat# 3652), anti-cyclin D1 (Cat# 2922), anti-cyclin E1 (Cat# 4129), anti-cyclin B1 (Cat# 12231), anti-p-*JNK* (Thr183/Tyr185, Cat# 4668), anti-*JNK* (Cat# 9252), anti-p38 MAPK (Cat# 8690), anti-p-p38 MAPK (Thr180/Tyr182, Cat# 4511), and anti-E2F1 (Cat# 3742) were purchased from Cell Signaling Technology, anti-*CHK1* (Cat# sc-8408) and anti-*CDC2* (Cat# sc-954) were purchased from Santa Cruz Biotechnology (Dallas, TX, USA), and anti-*GAPDH* (Cat# KC-5G4) was purchased from (KangChen Bio-tech, Shanghai, China). The horseradish peroxidase-conjugated secondary antibodies anti-rabbit (Cat# NA934) and anti-mouse (Cat# NA931) IgG were purchased from GE Healthcare (Little Chalfont, UK). An anti-AGO2 antibody (Cat# RN003M) used for miRNA ribonucleoprotein complex immunoprecipitation (miRNA-IP) assays was purchased from MBL (Nagoya, Aichi, Japan). An anti-E2F1 antibody (Cat# 17-10061) used for chromatin immunoprecipitation (ChIP) assays was purchased from Merck Millipore (Burlington, MA, USA). Anti-*PRKCD* (Cat# sc-8402) and anti-*WEE1* (Cat# 13084) antibodies used for IHC were purchased from Santa Cruz and Cell Signaling Technology, respectively.

### 2.3. Cell lines

The ESCC cell lines KYSE-410 and KYSE-510 were obtained from DSMZ, the German Resource Center for Biological Materials [19], and cultured in Dulbecco's modified Eagle's medium (Life Technologies/

Thermo Fisher Scientific; Cat# C11995500BT) supplemented with 10% fetal bovine serum (Life Technologies/Thermo Fisher Scientific; Cat# 10270). The immortalized esophageal epithelial cell line NE1 was provided by Professor GS Tsao (The University of Hong Kong) and cultured in EpiLife medium with 60  $\mu$ M calcium (Life Technologies/Thermo Fisher Scientific; Cat# MEPI500CA) mixed with defined keratinocyte-SFM (Life Technologies/Thermo Fisher Scientific; Cat# 10744019). All cell lines were cultured in a humidified incubator containing 5% CO<sub>2</sub> at 37 °C.

#### 2.4. Vectors, lentiviral transduction, and transfection

Lentiviral constructs expressing miRZip-424 (System Biosciences, Palo Alto, CA, USA; Cat# MZIP424-PP-1), which knocks down *miR-424* functionally, lenti-*miR-424* (System Biosciences; Cat# PMIRH424PP-1), which expresses the *miR-424* precursor, or the corresponding controls (System Biosciences; Cat# MZIP000-PP-1 and PMIRH000PP-1) were packaged using the ViraPower Lentiviral Packaging Mix (Life Technologies/Thermo Fisher Scientific; Cat# K497500) in 293FT cells, respectively. Stable cell lines expressing miRZip-424, lenti-*miR-424*, or the corresponding controls were generated via lentiviral transduction and selected with puromycin or by flow cytometry sorting for GFP positive populations. Small interfering RNAs (siRNAs) targeting *E2F1* and a scrambled control were purchased from RiboBio Co., Ltd. (Guangzhou, China; Cat# stQ0001999-1). Transfection of siRNA or plasmids was conducted using Lipofectamine 2000 reagent (Life Technologies/Thermo Fisher Scientific; Cat# 11668019) according to the manufacturer's instructions. The shRNA and siRNA sequences are presented in Supplementary Table S1.

#### 2.5. RNA isolation, miRNA microarray, and qRT-PCR analysis

For the 30 ESCC and ten NE tissue samples used for miRNA profiling analysis, total RNA was isolated using the mirVana miRNA Isolation Kit (Life Technologies/Thermo Fisher Scientific; Cat# AM1561). Human miRNA microarrays based on miRBase Release 18.0 (Agilent Technologies, Santa Clara, CA, USA; Cat# G4872A) were adopted for miRNA expression profiling analysis. Genespring 12.0 (Agilent Technologies) software was used to analyze the microarray data. Student's *t*-test for unpaired samples was used to identify differentially expressed miRNAs between ESCC and NE samples. Hierarchical clustering was performed using the Pearson centered correlation as a distance metric and the average linkage algorithm based on significantly different genes to combine cluster branches.

For the tissue and cell samples used for qRT-PCR analysis, total RNA was extracted using TRIzol reagent (Life Technologies/Thermo Fisher Scientific; Cat# 15596018). TaqMan *miR-424* (Assay ID: 000604, Life Technologies/Thermo Fisher Scientific; Cat# 4427975) qRT-PCR analysis was performed as described previously [18] with *RNU6B* (Assay ID: 001093, Life Technologies/Thermo Fisher Scientific; Cat# 4427975) as an internal control. For qRT-PCR analyses of pri-*miR-424*, pre-*miR-424*, and mRNAs, total RNA was reverse transcribed into cDNA using a RevertAid First Strand cDNA Synthesis Kit (Life Technologies/Thermo Fisher Scientific; Cat# K1621). PCR amplification of pri-*miR-424* was then performed using the TaqMan pri-miRNA assay kit (Assay ID: Hs03303697\_pri, Life Technologies/Thermo Fisher Scientific; Cat# 4427012) and the TaqMan Universal PCR Master Mix (Life Technologies/Thermo Fisher Scientific; Cat# 4304437), with GAPDH (Assay ID: 4333764, Life Technologies/Thermo Fisher Scientific; Cat# 4333764T) as an internal control. PCR amplification of pre-*miR-424* and mRNAs was performed using Power SYBR Green PCR Master Mix (Life Technologies/Thermo Fisher Scientific; Cat# 4367660) with GAPDH as an internal control. The specific primers used for qRT-PCR are presented in Supplementary Table S1. All PCR analyses were performed in a Light Cycler 480 thermocycler (Roche Diagnostics, Indianapolis, IN, USA).

qRT-PCR for each gene was performed in triplicate. Relative gene expression was analyzed using the 2<sup>- $\Delta$ CT</sup> method [20].

#### 2.6. Cell proliferation in vitro

For growth curve measurements, KYSE-410 and KYSE-510 cells stably expressing lenti-*miR-424*, miRZip-424, or the corresponding control vectors and NE1 cells transduced with lenti-*miR-424* or the control vectors for 3 days were prepared as single-cell suspensions and seeded in 96-well plates. The cell proliferation rate was detected using a CCK-8 cell proliferation kit (Dojindo, Minato-ku, Tokyo, Japan; Cat# CK04). For the colony formation assay, 200 cells were seeded into 6-well plates. After ten days of culture, the surviving colonies (>50 cells/colony) were counted with 1% crystal violet staining. Three independent experiments were performed.

#### 2.7. Tumor formation in nude mice

All animal experiments were performed according to the guidelines of the Council on Animal Care and approved by Sun Yat-sen University. Female BALB/c nude mice, aged 4–5 weeks, were purchased from Beijing Vital River Laboratory Animal Technology Co., Ltd. A total of 6  $\times$  10<sup>6</sup> KYSE-410 and KYSE-510 cells stably expressing miRZip-424 or the control vectors were injected subcutaneously into the dorsal flanks of nude mice. Each group contained five mice. Tumor size was measured every 3 days. After 5–6 weeks, the mice were killed, and the tumors were dissected. Tumor volumes were calculated as follows: volume = (D  $\times$  d<sup>2</sup>)/2, where D is the longest diameter and d is the shortest diameter.

#### 2.8. Cell synchronization and cell cycle assay by flow cytometry

ESCC cells stably expressing lenti-*miR-424*, miRZip-424, or the corresponding control vectors were synchronized in G<sub>0</sub>/G<sub>1</sub>-phase by serum starvation, at the onset of S-phase using a double-thymidine block (2 mM), or in mitosis with 100 ng/ml nocodazole treatment for 20 h as described previously [21]. The cells were collected at the indicated time points after release from synchronization, fixed in 70% ethanol, and stained with 50  $\mu$ g/ml propidium iodide. If further discrimination between G<sub>2</sub>-phase and M-phase was required, the fixed cells were stained with rabbit anti-pHH3 (Ser10) antibody and a secondary antibody conjugated with Alexa Fluor 647, followed by propidium iodide staining. The cell cycle distribution was monitored with a Gallios flow cytometer (Beckman Coulter, Brea, CA, USA) and analyzed with FlowJo v10.

#### 2.9. Western blotting

Cells were lysed in ice-cold lysis buffer with 1 $\times$  protease inhibitor cocktail (Roche Diagnostics; Cat# 4693116001) and 1 $\times$  phosphatase inhibitor cocktail 2 (Sigma-Aldrich; Cat#P5726) and 3 (Sigma-Aldrich; Cat# P0044). Protein concentrations were determined using the Protein Assay Reagent (Bio-Rad Laboratories, Cat# 5000002). Cell lysates were subjected to electrophoresis on acrylamide gels with a proper concentration. Separated proteins were transferred onto PVDF membranes (Merck Millipore; Cat# IPVH00010) and probed with primary antibodies after blocking with 5% dried milk and secondary antibodies. The antigen-antibody complexes were visualized with ECL Western Blotting Substrate (Life Technologies/Thermo Fisher Scientific; Cat#32106) on a ChemiDoc Touch (Bio-Rad Laboratories, Hercules, CA, USA). The specific intensity of each protein band was measured by Image Lab (Bio-Rad Laboratories) software and expressed as the ratio of the optical density of the band for each protein to that of GAPDH.

### 2.10. 3'UTR cloning and luciferase assay

Oligonucleotide pairs of *PRKCD* and *WEE1* 3'UTRs containing predicted binding sites for *miR-424* (Supplementary Table S1) were synthesized, annealed, and ligated into the pmirGLO Dual-Luciferase miRNA target expression vector (Promega, Madison, WI, USA; Cat# E1330). HEK293 cells were transfected with the luciferase reporter plasmid plus lenti-*miR-424* or miRZip-424. After 48 h, luciferase activities were assessed using the Dual-Luciferase 1000 Assay System (Promega; Cat# E1980) by measuring the luminescence signal in a GLOMAX luminometer (Promega). The experiments were performed in triplicate and repeated three times with negative controls.

### 2.11. miRNA-IP assay

KYSE-410 and KYSE-510 cells stably expressing *miR-424* precursor or control vectors were collected after release from G0/G1-phase for 12 h or from S-phase onset for 9 h. miRNA-IP assays of the collected cells were performed using the RiboCluster Profile RIP-Assay kit for microRNA (MBL; Cat# RN1005) following the manufacturer's protocol with Protein A Plus Agarose (Life Technologies/Thermo Fisher Scientific; Cat# 22180) and an anti-AGO2 antibody. RNA isolated from the immune complex of miRNA-IP was used for cDNA synthesis. qRT-PCR was performed to determine *PRKCD*, *WEE1* and *circLARP4* enrichment in the RNA-induced silencing complex (RISC); the average values of RISC-associated *GAPDH*, *B2M*, and *GUSB* were used for normalization [22]. The primers used for qRT-PCR of miRNA-IP product are presented in Supplementary Table S1. Data are presented as the  $2^{-\Delta\Delta C_p}$ , where  $\Delta C_p = C_{pRIP} - C_{pInput}$ , and  $\Delta\Delta C_p = \Delta C_p - \Delta C_{pControl}$ .

### 2.12. ChIP assay

KYSE-410 cells were collected after release from G0/G1 for 8 h. ChIP assay of the collected cells were performed using the EZ-Magna ChIP HiSens Kit (Merck Millipore, Burlington, MA, USA; Cat# 17-10461) according to the manufacturer's instructions with an anti-E2F1 antibody. ChIP DNA enrichment was analyzed by qRT-PCR using primers presented in Supplementary Table S1. Data are presented as  $2^{-\Delta\Delta C_p}$ , where  $\Delta C_p = C_{pChIP} - C_{pInput}$ , and  $\Delta\Delta C_p = \Delta C_p - \Delta C_{pNegative}$ . The quantification of DNA enrichment in the *CDC2* gene promoter was used as a positive control, and *GAPDH* was used as a negative control.

### 2.13. miR-424 promoter cloning and luciferase assay

A 1750-bp putative promoter sequence that contained a portion of pri-*miR-424* and was therefore located upstream of *miR-424* was synthesized and cloned into the pEZ-LvPG04 lentiviral reporter vector (GeneCopoeia, Rockville, MD, USA). A QuickChange Site-Directed Mutagenesis kit (Agilent Technologies; Cat# 210518) was used to mutagenize the E2F1 binding sites with the primers presented in Supplementary Table S1. KYSE-410 cells were infected with the lentiviral particles and selected with puromycin. The luciferase activities were assessed using a Secrete-Pair Dual Luminescence assay kit (GeneCopoeia, Cat# LF031).

### 2.14. IHC

IHC was performed using the standard peroxidase anti-peroxidase complex method. Briefly, FFPE sections were deparaffinized and rehydrated. Peroxidase inactivation and antigen retrieval were achieved by incubating samples in 3% H<sub>2</sub>O<sub>2</sub> and EDTA buffer. The primary antibodies used were PRKCD (1:40 dilution) and WEE1 (1:100 dilution). Immunoperoxidase staining was carried out using peroxidase-conjugated polymer solution (ZSGB-Bio, Beijing, China; Cat# PV6000). Then the slides were visualized with 3,3'-diaminobenzidine (ZSGB-Bio; Cat# ZLI-9017) and counterstained with hematoxylin.

A pathologist blinded to the clinicopathological information performed the evaluation of PRKCD and WEE1 protein expression by using a semi-quantitative system as described previously [23].

### 2.15. Statistical analysis

Calculations of the mean value  $\pm$  standard deviation (SD) were based on three independent experiments. Data analyses, except for microarray analysis, were carried out using the SPSS 22.0 statistics package (IBM, Armonk, NY, USA). Continuous variables were analyzed using Student's *t*-test. Repeated measures ANOVA was performed to assess the statistical significance of cell growth curves and tumor growth in nude mice. The correlations between *miR-424* expression and the expression of target proteins or clinicopathological parameters were analyzed by the Chi-square test. Overall survival was defined as the time from surgery to death, and patients who were still alive at the time of last follow-up were censored. Survival curves were analyzed by the Kaplan-Meier method and the log-rank test. The Cox proportional hazards regression model was used to identify independent prognostic factors. A two-tailed  $p < 0.05$  was considered statistically significant.

### 2.16. Data sharing

The dataset for the miRNA microarray analysis is available in the Gene Expression Omnibus repository under accession number GSE114110.

## 3. Results

### 3.1. miR-424 is upregulated in ESCC and correlates with poor prognosis

To identify ESCC-related miRNAs, miRNA arrays were used to analyze 30 ESCC and ten NE samples. A total of 37 miRNAs were identified as differentially expressed miRNAs between the two groups (fold change  $>3$ ,  $p < 0.001$  by Student's *t*-test with the Benjamin-Hochberg correction, Fig. 1a). *miR-424* was one of 12 miRNAs that were upregulated in ESCC samples compared with NE samples (Fig. 1a). The expression level of *miR-424* was further evaluated in 60 pairs of ESCC specimens and their matched NE samples by qRT-PCR. The results showed that *miR-424* expression was significantly elevated in ESCC specimens compared with that in normal counterparts ( $p < 0.001$  by Student's *t*-test for paired samples, Fig. 1b).

To evaluate whether the upregulation of *miR-424* correlates with clinical ESCC progression, we examined *miR-424* expression by qRT-PCR in a cohort of 190 Stage IB-IIIC ESCC patients who underwent radical surgery with no neoadjuvant or adjuvant treatment. The expression of *miR-424* was classified as high or low according to the median *miR-424* expression value of the whole cohort. There were no statistically significant associations between *miR-424* expression and patients' clinicopathological factors ( $p > 0.05$  by Chi-square test, Table 1). However, both univariate and multivariate survival analyses revealed that high *miR-424* expression was significantly associated with poor patient prognosis ( $p < 0.05$  by Kaplan-Meier method with log-rank test for univariate survival analysis and Cox's proportional hazards regression analysis for multivariate survival analysis, Fig. 1c; Tables 2 and 3).

### 3.2. miR-424 promotes ESCC cell proliferation

To investigate the biological function of *miR-424*, the ESCC cell lines KYSE-410 and KYSE-510 were transduced with lentiviruses expressing lenti-*miR-424*, miRZip-424, or the corresponding control vectors and further selected to generate stable *miR-424*-overexpressing or *miR-424*-knockdown ESCC cells. In addition, the immortalized esophageal epithelial cell line NE1 was freshly transduced with lentiviruses expressing lenti-*miR-424* and control vectors. Lenti-*miR-424* transduction

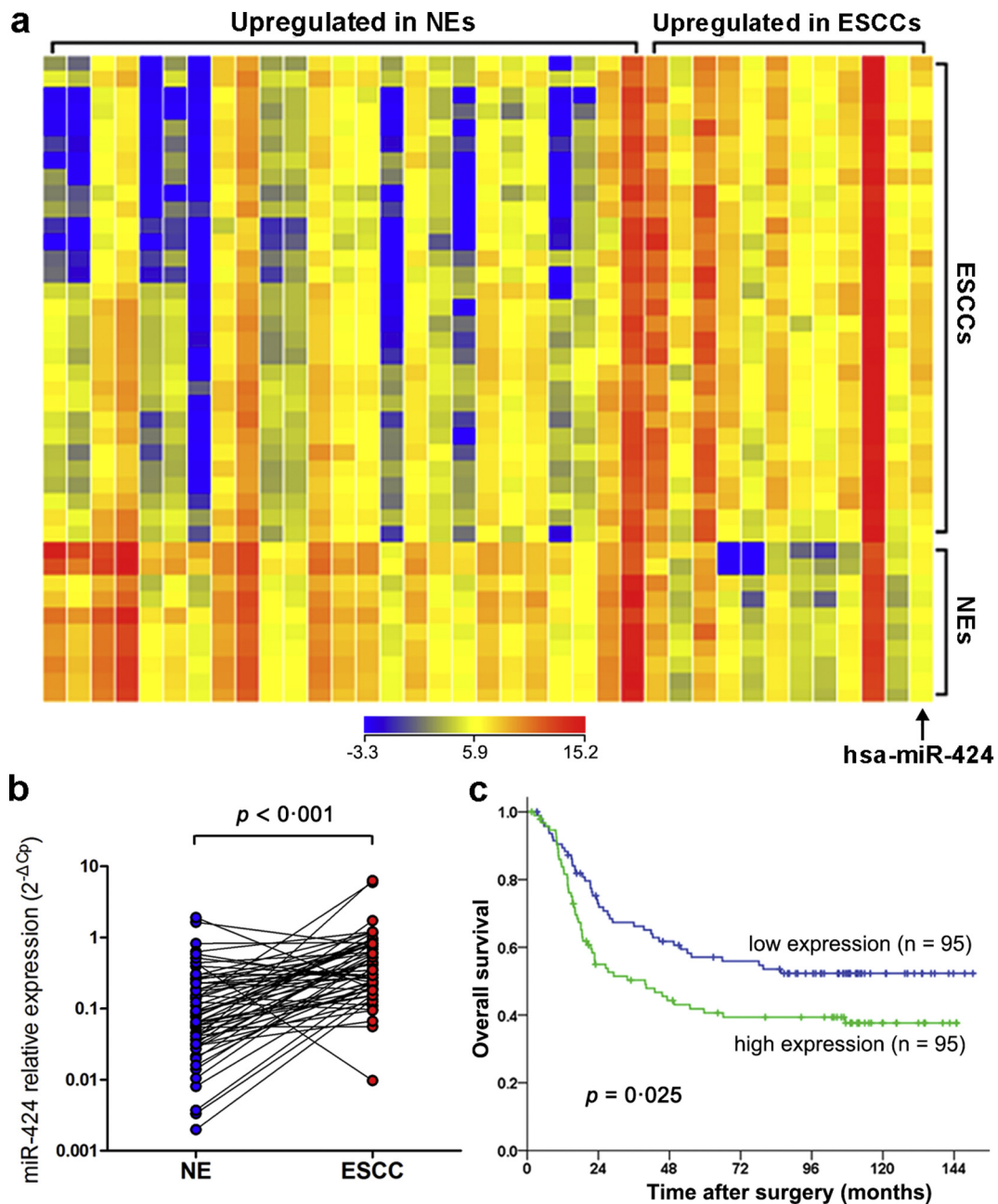


**Fig. 1.** *miR-424* is upregulated in ESCC and correlates with poor prognosis. (a) Hierarchical cluster analysis showed differential miRNA expression profiles between 30 ESCC and ten NE samples (fold change  $>3$ ,  $p < 0.001$  by Student's *t*-test with the Benjamin-Hochberg correction). Each column represents a miRNA, and each row represents a specimen. Blue and red denote genes that are under- and overexpressed, respectively. (b) qRT-PCR verified the upregulation of *miR-424* in 60 ESCC specimens compared with the expression seen in normal counterparts ( $p < 0.001$  by Student's *t*-test for paired samples). (c) Kaplan-Meier analysis showed that the overall survival ( $p = 0.025$  by log-rank test) of ESCC patients with high *miR-424* expression was poorer than that of patients with low *miR-424* expression.

significantly increased *miR-424* expression in KYSE-410, KYSE-510, and NE-1 cells compared with control vectors (Fig. 2a). As miRZip anti-miRNA lentivectors exhibit anti-miRNA activity without directly decreasing miRNA expression [24], we did not determine *miR-424* expression after miRZip-424 transduction.

Cell growth curves and colony formation assays were performed to explore the effect of *miR-424* on ESCC cell proliferation *in vitro*. As shown in Fig. 2b, *miR-424* overexpression significantly promoted KYSE-410, KYSE-510, and NE1 cell growth, whereas *miR-424* knockdown significantly retarded the growth rate of KYSE-410 and KYSE-510 cells (Fig. 2b). Colony formation assays also showed that *miR-424*-knockdown in KYSE-410 and KYSE-510 cells results in fewer and smaller colonies than were produced by control cells, whereas the

opposite results were observed after overexpressing *miR-424* in KYSE-410 and KYSE-510 cells (Fig. 2c).

The *in vivo* tumorigenic ability of *miR-424* was investigated with a tumor xenograft experiment by subcutaneous injection of KYSE-410 and KYSE-510 cells stably expressing miRZip-424 or the control vector into nude mice. As shown in Fig. 2d, the tumors formed by *miR-424*-knockdown KYSE-410 or KYSE-510 cells were smaller than the tumors formed by control cells.

### 3.3. Role of *miR-424* in ESCC cell cycle progression

The loss of normal cell cycle control is one of the factors that induces sustained cell proliferation [5]. As *miR-424* promotes ESCC cell

**Table 1**  
Association between *miR-424* expression and clinicopathological characteristics in 190 esophageal squamous cell carcinoma patients.

Variables	<i>miR-424</i> expression in primary tumors			p value <sup>a</sup>
	Cases	Low (%)	High (%)	
Gender				0.095
Male	142	76 (53.5)	66 (46.5)	
Female	48	19 (39.6)	29 (60.4)	
Age (years)				0.384
≤59 <sup>b</sup>	98	52 (53.1)	43 (46.9)	
>59	92	46 (46.7)	49 (53.3)	
Tumor location				1.000
Upper	34	17 (50.0)	17 (50.3)	
Middle	102	51 (50.0)	51 (50.0)	
Lower	54	27 (50.0)	27 (50.0)	
Histological differentiation				0.340
Well	48	26 (54.2)	22 (45.8)	
Moderate	96	43 (44.8)	53 (55.2)	
Poor	46	26 (56.5)	20 (43.5)	
T stage				0.401
T1–2	47	26 (55.3)	21 (44.7)	
T3–4	143	69 (48.3)	74 (51.7)	
N stage				0.146
N0	100	45 (45.0)	55 (55.0)	
N1–3	90	50 (55.6)	40 (44.4)	
TNM stage				0.450
Stage I	15	9 (60.0)	6 (40.0)	
Stage II	92	42 (45.7)	50 (54.3)	
Stage III	83	44 (53.0)	39 (47.0)	

<sup>a</sup> Chi-square test.  
<sup>b</sup> Mean age.

proliferation, we next focused our attention on understanding whether and how *miR-424* affects ESCC cell cycle progression.

First, KYSE-410 and KYSE-510 cells stably expressing miRZip-424, lenti-*miR-424*, or the corresponding control vectors were synchronized

**Table 2**  
Univariate analysis of *miR-424* expression level and clinicopathological factors for overall survival and disease-free survival in 190 surgically resected esophageal squamous cell carcinoma patients.

Variables	Cases	Overall survival (months)	
		Median	p value <sup>a</sup>
Gender			0.622
Male	142	66.1	
Female	48	40.1	
Age (years)			0.772
≤59 <sup>b</sup>	98	65.8	
>59	92	44.5	
Tumor location			0.578
Upper	34	NR <sup>c</sup>	
Middle	102	47.2	
Lower	54	66.1	
Histological differentiation			< 0.001
Well	48	NR	
Moderate	96	107.3	
Poor	46	23.4	
T stage			0.146
T1–2	47	NR	
T3–4	143	49.5	
N stage			< 0.001
N0	100	NR	
N1–3	90	21.7	
TNM stage			< 0.001
Stage I	15	NR	
Stage II	92	NR	
Stage III	83	21.5	
<i>miR-424</i>			0.025
Low expression	95	NR	
High expression	95	39.8	

<sup>a</sup> Kaplan-Meier method, log-rank test.  
<sup>b</sup> Median age.  
<sup>c</sup> Not reached.

**Table 3**  
Multivariate analysis for overall survival and disease-free survival in surgically resected esophageal squamous cell carcinoma patients.

Variable	Overall survival		
	p value <sup>a</sup>	HR	95.0% CI for HR
<i>miR-424</i> expression	0.001	2.040	1.356–3.069
Histological differentiation	0.008	1.533	1.120–2.099
N stage	<0.001	3.514	2.268–5.444

Abbreviations: HR hazard ratio, CI confidence interval.  
<sup>a</sup> Cox's proportional hazards regression analysis (Forward stepwise).

in G0/G1-phase by serum withdrawal. The cells were then switched to a standard culture medium to allow the cells to re-enter the cell cycle. KYSE-410-miRZip-424 cells displayed an increased percentage of cells in G1-phase and a decreased percentage of cells in S-phase compared with KYSE-410-miRZip-Control cells, whereas KYSE-410-lenti-*miR-424* cells exhibited a decreased percentage of cells in G1-phase and an increased percentage of cells in S-phase compared with KYSE-410-lenti-miR-Control cells (Fig. 3a). However, no obvious difference was observed between KYSE-510-miRZip-424 and KYSE-510-miRZip-Control or between KYSE-510-lenti-*miR-424* and KYSE-510-lenti-miR-Control cells after release from G0/G1-phase (Supplementary Fig. 1a), suggesting that *miR-424* affects the G1/S transition in KYSE-410 cells but not KYSE-510 cells.

Next, the effect of *miR-424* on S-phase and G2/M-phase progression in ESCC cells was determined. KYSE-410 and KYSE-510 cells stably expressing miRZip-424, lenti-*miR-424*, or the corresponding control vectors were synchronized at the onset of S-phase by double-thymidine block, and the cells were then released and harvested at sequential time points for the measurement of S-phase and G2/M-phase events. In KYSE-410 cells, approximately 80% of miRZip-424, lenti-*miR-424*, and the corresponding control cells were synchronized in G1-phase, and 20% were initially in S-phase. After releasing the cells for 2 h, almost all cells were in S-phase; the cells then gradually entered G2/M-phase, with a peak for G2/M-phase cells at 6 h after release. No significant differences in cell cycle distribution among miRZip-424, lenti-*miR-424*, and the corresponding control cells were observed during the first 6 h after release from the onset of S-phase (Fig. 3b), indicating that *miR-424* did not affect S-phase progression. Later, however, the KYSE-410-miRZip-424 cells displayed an increased percentage of cells in G2/M-phase but a decreased percentage of cells in G1-phase compared with control cells at 8, 10, and 12 h after release from the onset of S-phase, whereas the opposite results were obtained in KYSE-410-lenti-*miR-424* cells compared with control cells. These observations suggest that *miR-424*-knockdown or overexpression respectively blocked or promoted the G2/M cell cycle progression of KYSE-410 cells (Fig. 3b). Similar results were observed in KYSE-510 cells (Supplementary Fig. 1b).

To further discriminate between G2- and M- phase cells, stable KYSE-410-miRZip-424, KYSE-410-lenti-*miR-424*, and the corresponding control cells were enriched at the onset of S-phase and then released with bivariate analysis of phospho-histone H3 (pHH3, Ser10) expression, a mitosis-specific marker, versus DNA content. As shown in Fig. 3c, after releasing cells from the onset of S-phase for 8–10 h, a greater percentage of *miR-424*-knockdown but a smaller percentage of *miR-424*-overexpressing cells remained in G2-phase (pHH3-negative cells) than were observed with control cells, suggesting a role of *miR-424* in G2/M transition. However, when mitotic cells were enriched by nocodazole arrest and released, KYSE-410-miRZip-424, KYSE-410-lenti-*miR-424*, and the corresponding control cells exhibited similar rates of reduction of the mitotic population (pHH3-positive cells) (Supplementary Fig. 2). These results indicated that the expression levels of *miR-424* affected G2/M but not mitotic transition in ESCC cells.

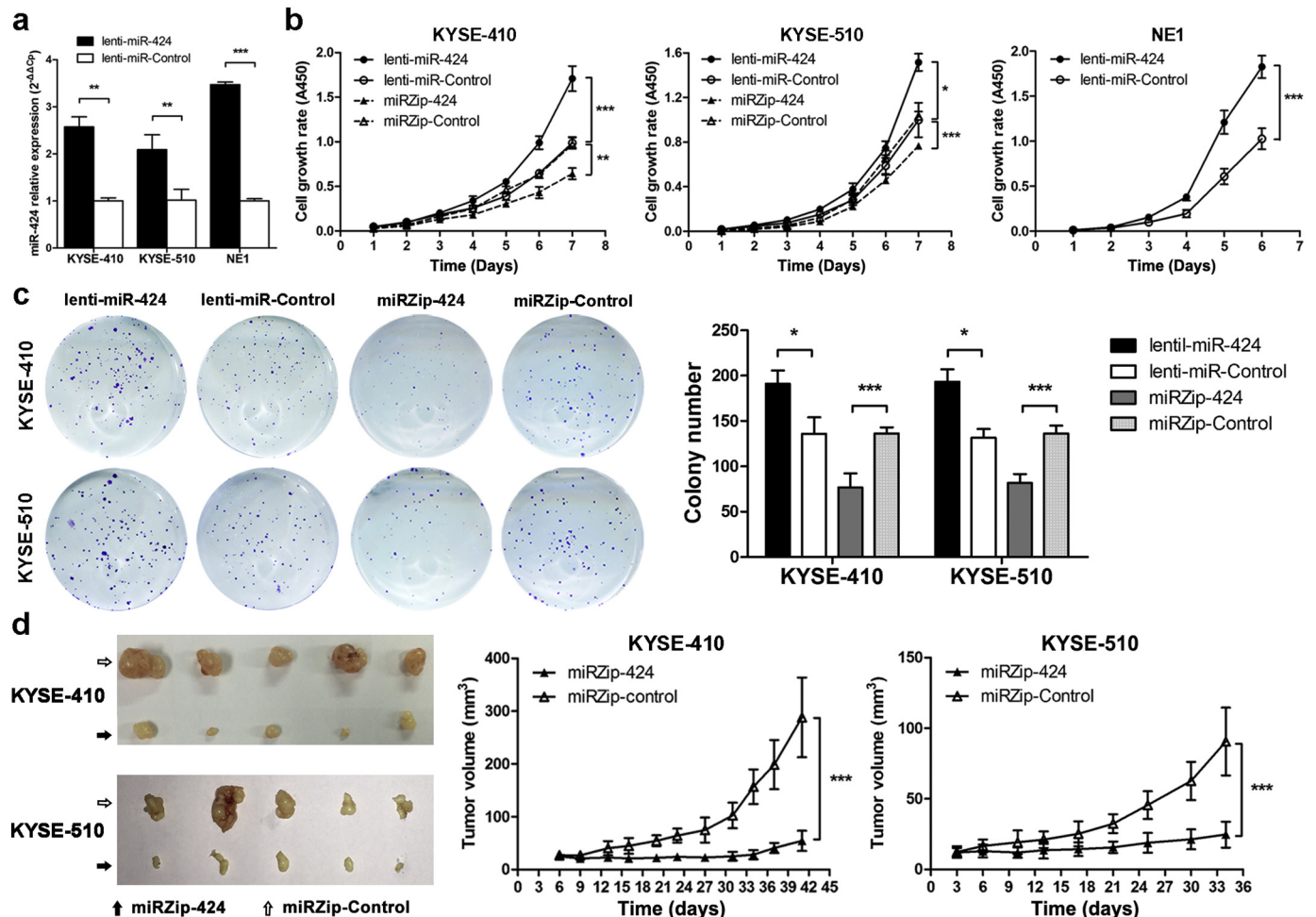


**Fig. 2.** *miR-424* promotes ESCC cell proliferation *in vitro* and *in vivo*. (a) qRT-PCR analyses showed the relative *miR-424* expression levels in KYSE-410 and KYSE-510 ESCC cells and NE1 immortalized esophageal epithelial cells expressing the *miR-424* precursor (lenti-*miR-424*) or control vectors. Data are presented as the mean  $\pm$  SD of three independent experiments. \*\*,  $p < 0.01$  or \*\*\*,  $p < 0.001$  by Student's *t*-test for unpaired samples. (b) Cell growth curves were generated for *miR-424*-overexpressing (lenti-*miR-424*) or *miR-424*-knockdown (miRZip-424) KYSE-410, KYSE-510, and NE1 cells with a CCK-8 cell proliferation kit. Data are presented as the mean  $\pm$  SD of three independent experiments. \*,  $p < 0.05$ ; \*\*,  $p < 0.01$ ; or \*\*\*,  $p < 0.001$  by repeated measures ANOVA. (c) Representative images and results of colony formation assays of KYSE-410 and KYSE-510 cells expressing *miR-424*-knockdown (miRZip-424), *miR-424*-overexpressing, or the corresponding control vectors. Data are presented as the mean  $\pm$  SD of three independent experiments. \*\*\*,  $p < 0.001$  by Student's *t*-test for unpaired samples. (d) Tumor xenograft experiments with subcutaneous injection of KYSE-410 or KYSE-510 cells stably expressing miRZip-424 or control vectors into nude mice ( $n = 5$  in each group) demonstrated the *in vivo* tumorigenic ability of *miR-424*. Images of tumor-bearing mice and tumors from all mice in each group are shown. Tumor volumes were measured on the indicated days, and each data point represents the mean  $\pm$  SD of five nude mice. \*\*\*,  $p < 0.001$  by repeated measures ANOVA.

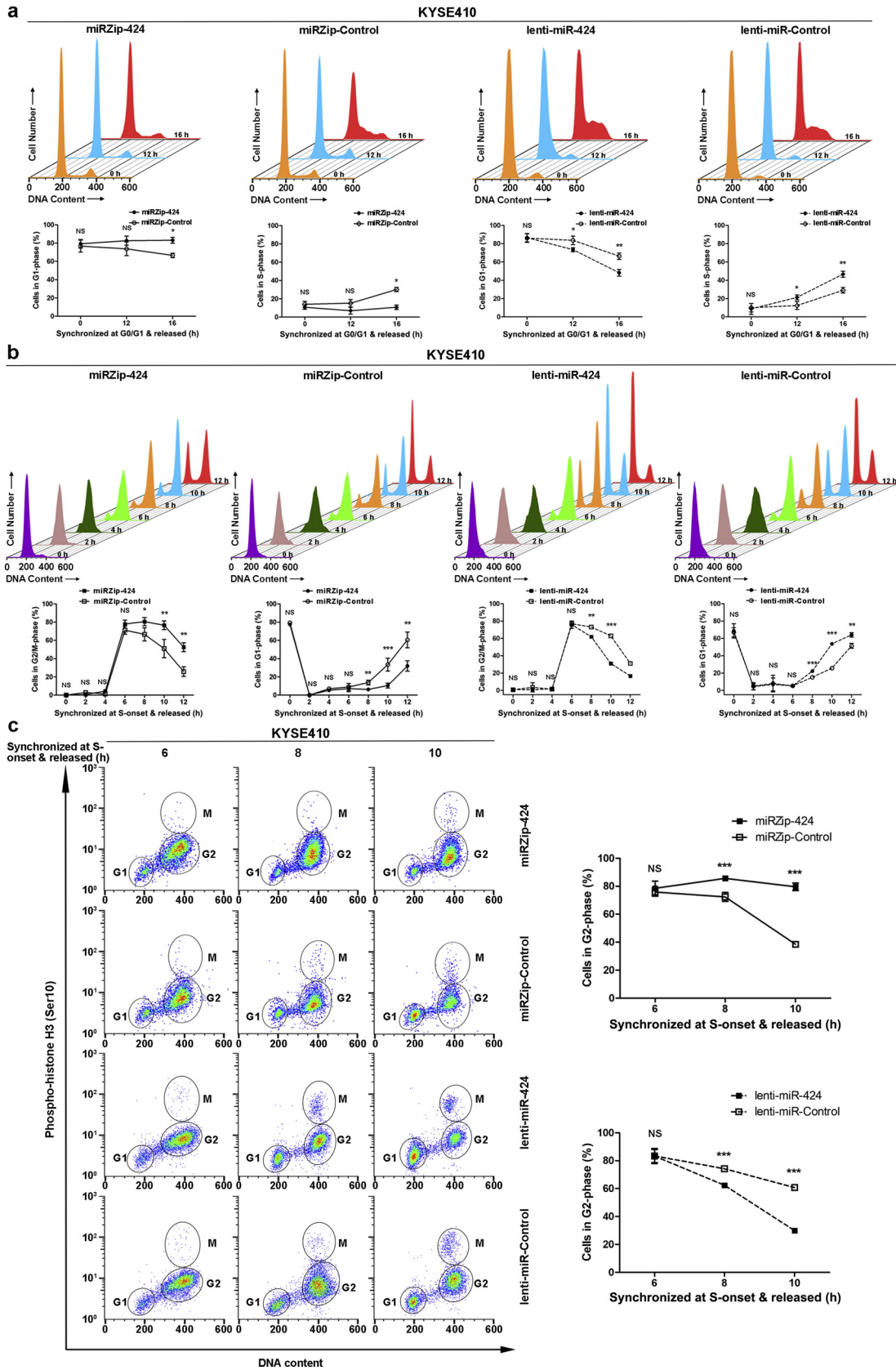
Taken together, the cell cycle analyses of ESCC cells after synchronization and release from different cell cycle phases provided evidence that knockdown or overexpression of *miR-424* respectively negatively or positively regulates G1/S transition in KYSE-410 cells and G2/M transition in both KYSE-410 and KYSE-510 cells.

### 3.4. *miR-424* expression is transcriptionally regulated by *E2F1* during G1/S transition

As *miR-424* functions in cell cycle progression, we evaluated the expression of *miR-424* in various cell cycle phases. qRT-PCR analyses

showed that *miR-424* expression increased 12 or 16 h after release from G0/G1-phase in both KYSE-410 and KYSE-510 cells (Fig. 4a), suggesting that *miR-424* expression increased with cell cycle progression from G0/G1 to S-phase. However, the expression of *miR-424* did not show obvious changes during G2/M progression (Supplementary Fig. 3). A small increase in *miR-424* expression was observed after release from the onset of S-phase for 10 h (Supplementary Fig. 3), which might be due to increased *miR-424* expression during G1/S transition, as some of the cells have already left G2/M-phase and re-entered G1/S-phase as a part of a new division cycle at this time point as shown in Fig. 3b and Supplementary Fig. 1b.

**Fig. 3.** Effects of *miR-424* expression on G1/S and G2/M cell cycle progression in KYSE-410 ESCC cells. (a) Stable *miR-424*-knockdown (miRZip-424), *miR-424*-overexpressing (lenti-*miR-424*), and the corresponding control KYSE-410 cells were synchronized in G0/G1-phase by serum starvation and released, and the cell cycle distribution was monitored by flow cytometry at the indicated time points with propidium iodide staining. Representative images of the cell cycle distribution (upper) and the percentage of cells in G1-phase or S-phase (lower) are shown. (b) Stable *miR-424*-knockdown (miRZip-424), *miR-424*-overexpressing (lenti-*miR-424*), and the corresponding control KYSE-410 cells were synchronized at the onset of S-phase by double-thymidine block and released, and the kinetic transition of the cells through S-phase to G2/M-phase was monitored by flow cytometry at the indicated time points with propidium iodide staining. Representative images of the cell cycle distribution (upper) and the percentage of cells in G2/M- or G1-phase (lower) are shown. (c) Stable *miR-424*-knockdown (miRZip-424), *miR-424*-overexpressing (lenti-*miR-424*), and the corresponding control KYSE-410 cells were synchronized at the onset of S-phase by double-thymidine block and released, and the kinetic transition of the cells through G2-phase to M-phase was monitored by flow cytometry at the indicated time points with propidium iodide and anti-pH3 and Alexa Fluor 647-conjugated secondary antibody double-staining. Representative images of the cell cycle distribution (left) and the percentage of cells in G2-phase (right) are shown. All the data are presented as the mean  $\pm$  SD of three independent experiments. \*,  $p < 0.05$ ; \*\*,  $p < 0.01$ ; \*\*\*,  $p < 0.001$ ; or NS, not significant by Student's *t*-test for unpaired samples.



The biogenesis of miRNA is a multistep process. miRNA genes are first transcribed into pri-miRNAs and subjected to a preliminary processing step to form hairpin-loop RNAs (pre-miRNAs), which are then exported to the cytoplasm and cleaved to produce mature miRNAs [25]. In our ESCC cells, qRT-PCR amplification confirmed the upregulation of pri-*miR-424* and pre-*miR-424* in KYSE-410 and KYSE-510 cells after release from G0/G1-phase (Fig. 4a). Kinetic studies revealed that the increases in pri-*miR-424* and pre-*miR-424* levels happened before the increase in mature *miR-424* levels, suggesting that the elevated *miR-424* levels observed after release from G0/G1-phase were primarily due to *miR-424* gene transcription. Notably, the generation of mature *miR-424* led to reductions of pri-miRNA and pre-miRNA levels 12 h after release from G0/G1-phase. This effect could be due to the cleavage and degradation of the pri-miRNA after the pre-miRNA is excised, the existence of a negative regulatory feedback loop, or a combination of both mechanisms [26].

Llobet-Navas et al. [26] identified the transcription start site (TSS) of the *miR-424* gene, and a region located ~2 kb upstream of the TSS that is strongly enriched in active histone promoter marks could be the putative promoter region for its transcription. In the promoter region, two binding sites of E2F1 (–769 to –757 and –145 to –134), a widely studied transcription factor that activates the transcription of genes required for cell cycle entry and DNA synthesis [27], were identified using JASPAR [28] (Fig. 4b). As expected, knockdown of *E2F1* decreased the expression of pri-*miR-424*, pre-*miR-424*, and mature *miR-424* in ESCC KYSE-410 cells (Fig. 4c).

To confirm the direct binding between E2F1 and the *miR-424* promoter, a ChIP assay with 5 pairs of primers within the putative promoter region was performed to investigate the presence of E2F1 in the endogenous putative promoter in KYSE-410 cells 8 h after release from G0/G1-phase. The results revealed that the strongest enrichment of E2F1 happened in the two regions (P2 and P4) that contained the predicted E2F1-binding sites, and the levels were higher than those of the *bona fide* E2F1 target *CDC2* (Fig. 4d). In addition, the P4 region of the second E2F1-binding site was enriched more than the P2 region of the first E2F1-binding site.

To evaluate the role of the putative E2F1-binding sites in the upregulation of *miR-424* transcription during G1/S progression, a 1750-bp fragment of the putative promoter region encompassing the wild type or mutant E2F1 binding sites was inserted into pEZX-LvPG04, a GLuc-ON transcriptional response element lentiviral clone, using a secreted *Gaussia* luciferase (GLuc) as the reporter. This reporter was integrated into the genome of KYSE-410 cells by lentiviral delivery to create a pri-miR reporter cell line. After releasing the cells from G0/G1-phase for 8 h, the wild-type *miR-424* promoter exhibited significantly higher GLuc activity than the mutant promoters (Fig. 4e). Notably, the mutation of the second E2F1 binding site decreased the luciferase activity more than the mutation of the first binding site.

Taken together, these data demonstrated that E2F1 binds to the *miR-424* promoter and directly activates its transcription during the G1/S transition. In addition, the predicted second binding site of E2F1 might play a more important role than the first binding site during E2F1-mediated *miR-424* transcriptional activation.

### 3.5. *miR-424* directly targets *PRKCD* and *WEE1* in ESCC cells

The biological functions of miRNAs are mediated by their ability to directly interact with the 3'UTRs of target mRNAs and attenuate their expression. By searching publicly available algorithms (TargetScan and miRanda), we found a series of genes that are involved in cell cycle progression regulation and might be potential targets of *miR-424*. Among those genes, *PRKCD* [29], *CDC25A* [30], *PDCD4* [31], *LATS2* [32], *cyclin D1*, and *cyclin E1* [33] function primarily in G1/S transition, *CHK1* [34] functions primarily in S-phase DNA replication and G2/M transition [34], and *WEE1* [35] and *cyclin B1* [33] function primarily in G2/M transition.

We analyzed the impact of *miR-424* on the levels of the endogenous proteins encoded by the above potential target genes by synchronizing and releasing ESCC cells from G0/G1-phase or the onset of S-phase. During G1/S progression, western blotting revealed that knockdown of *miR-424* clearly elevated *PRKCD* protein in KYSE-410 (Fig. 5a) but not KYSE-510 (Supplementary Fig. 4a) cells. However, no obvious changes in *LATS2*, *PDCD4*, *CDC25A*, *cyclin D1*, and *cyclin E1* expression caused by *miR-424* knockdown were observed in either KYSE-410 (Fig. 5a) or KYSE-510 cells (Supplementary Fig. 4a). When the cells were released from the onset of S-phase, *WEE1* protein expression increased gradually during S-phase and G2-phase. In addition, this elevation was more pronounced in *miR-424*-knockdown cells than in control cells (Fig. 5b; Supplementary Fig. 4b). However, expression changes in two additional G2/M progression regulators, *CHK1* and *cyclin B1*, were not observed after knockdown of *miR-424* (Fig. 5b; Supplementary Fig. 4b). In addition, knockdown of *miR-424* did not induce changes in the expression of either *WEE1* protein during the G1/S transition (Fig. 5a) or *PRKCD* during the G2/M transition (Fig. 5b).

One fragment of the *PRKCD* 3'UTR and two fragments of the *WEE1* 3'UTR that contained the *miR-424*-binding sites predicted by bioinformatics algorithms were subcloned into the pmiRGLO dual-luciferase reporter vector (Fig. 5c). A luciferase assay showed that overexpression of *miR-424* attenuated the reporter activities driven by the 3'UTRs of *PRKCD* and *WEE1* transcripts, but knockdown of *miR-424* elevated these reporter activities. However, dysregulation of *miR-424* did not result in alterations in the reporter activities driven by the mutated 3'UTRs of these transcripts within the *miR-424*-binding-regions (Fig. 5d).

Next, we demonstrated the direct binding of *miR-424* to endogenous *PRKCD* and *WEE1* by immunoprecipitating Ago2, a core component of the RISC. Enrichment of the *PRKCD* transcript significantly increased in *miR-424*-overexpressing KYSE-410 cells after release from G0/G1 for 12 h, while *WEE1* enrichment increased in both *miR-424*-overexpressing KYSE-410 and KYSE-510 cells after release from the onset of S-phase for 9 h, compared with the levels in control cells, respectively (Fig. 5e). No enrichment of *PRKCD* was observed during G2/M progression, and no enrichment of *WEE1* was observed during G1/S progression. The results of the miRNP-IP assay were consistent with the above effects of *miR-424* on the cell cycle distribution and target gene expression, as shown by flow cytometry and western blotting, indicating that the effects of *miR-424* on target genes were cell cycle-phase specific. However, the reason why *miR-424* failed to target *PRKCD* during G1/S progression in KYSE-510 cells was unknown.

Mounting evidence has demonstrated that transcripts of non-coding RNAs (nc-RNAs) that contain miRNA-binding sites can act as natural miRNA sponges to affect the efficacy of miRNA target repression. *circLARP4*, which is localized in the cytoplasm, was identified previously as a natural sponge of *miR-424* and demonstrated to inhibit its activity by directly binding to *miR-424* [36]. In ESCC cells, our miRNP-IP assay proved that *circLARP4* could be enriched in *miR-424*-overexpressing KYSE-410 and KYSE-510 cells at G1/S transition, and the effect was more profound in KYSE-510 cells (Fig. 5e). Therefore, we supposed that *miR-424* was sponged by *circLARP4* in ESCC cells during G1/S transition, which could repress the ability of *miR-424* to bind to and target *PRKCD*. However, knockdown of *miR-424* had no influence on the expression of *circLARP4* (Supplementary Fig. 5).

Finally, we evaluated the expression levels of *PRKCD* and *WEE1* protein in ESCC and NE specimens by IHC analysis. Positive staining for *PRKCD* and *WEE1* was observed in the cytoplasmic and nuclear regions, respectively (Fig. 5f and Supplementary Fig. 6). The expression of *PRKCD* or *WEE1* protein of each specimen was classified as high or low according to the median protein expression value in the ESCC samples. Correlation studies showed that *miR-424* levels determined by qRT-PCR were significantly inversely correlated with the expression of *WEE1* ( $r = -0.282$ ,  $p = 0.003$  by Chi-square test) but not *PRKCD* ( $r = -0.179$ ,  $p = 0.061$  by Chi-square test, Fig. 5g) in the ESCC samples. However, no significant correlation between either *PRKCD* or

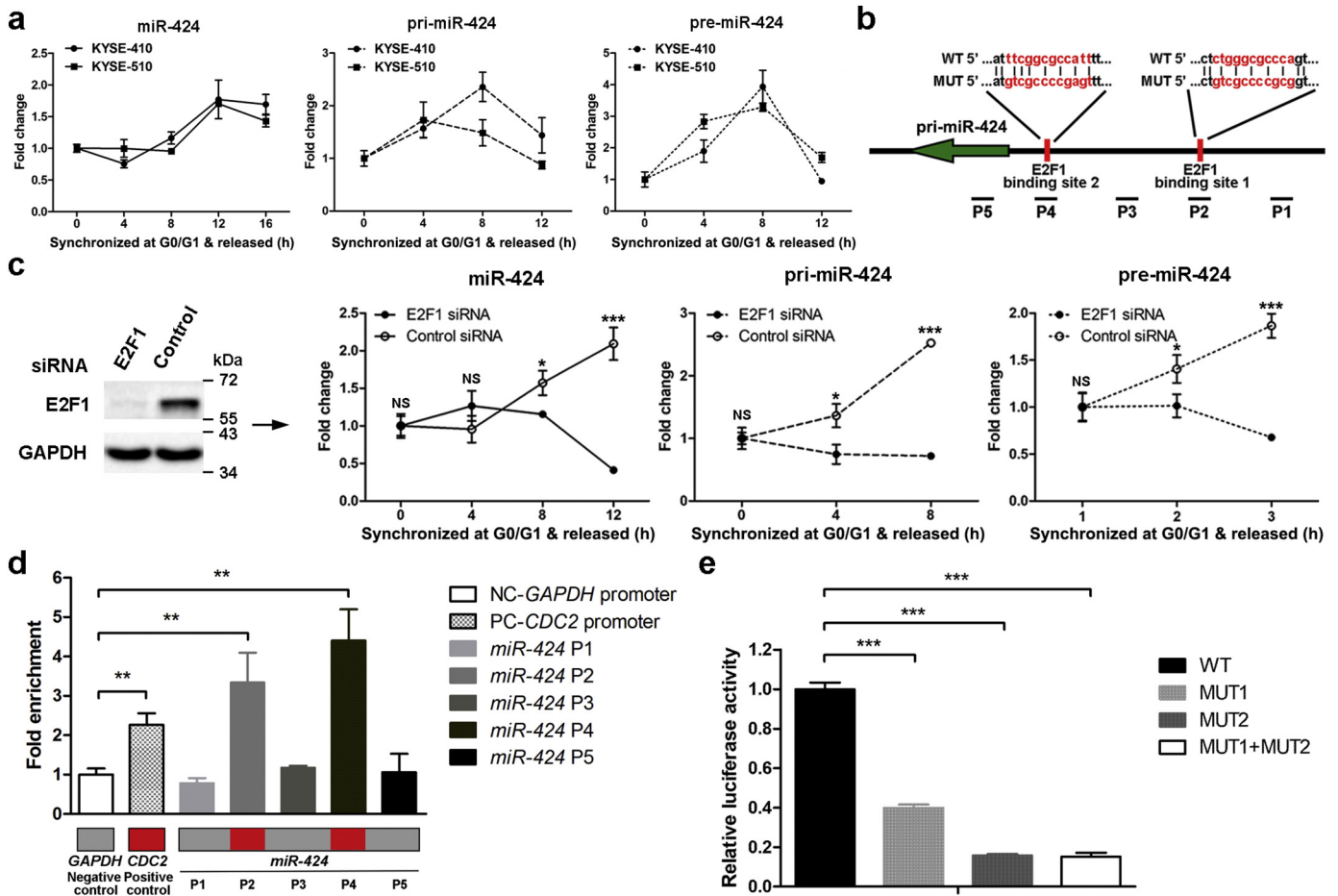


**Fig. 4.** Characterization of the *miR-424* promoter and transcriptional regulation of *miR-424* by E2F1 during G1/S transition. (a) KYSE-410 and KYSE-510 cells were synchronized in G0/G1-phase by serum starvation and released. qRT-PCR analysis shows the expression kinetics of *miR-424*, *pri-miR-424*, and *pre-miR-424* in KYSE-410 and KYSE-510 cells after release from G0/G1-phase for the indicated time points. Data are presented as the mean  $\pm$  SD of three independent experiments. (b) A schematic illustration shows two binding sites for E2F1 in the putative promoter region of the *miR-424* gene. Specific primers surrounding the promoter were designed. A fragment of the promoter region encompassing the wild-type or mutant E2F1 binding sites was cloned into a reporter vector. (c) Expression of E2F1 was silenced using siRNA (left panel). qRT-PCR showed changes in the expression kinetics of *miR-424*, *pri-miR-424*, and *pre-miR-424* after knocking down *E2F1* in KYSE-410 cells during G1/S transition (right panel). Data are presented as the mean  $\pm$  SD of three independent experiments. \*,  $p < 0.05$ ; \*\*\*,  $p < 0.001$ ; or NS, not significant by Student's *t*-test for unpaired samples to compare differences in expression between *E2F1*-knockdown and control cells at each time point. (d) ChIP was performed with an anti-E2F1 antibody on lysates of KYSE-410 cells after release from G0/G1-phase for 8 h. The quantification of genomic DNA enrichment was performed using specific primers surrounding the promoter, as shown in (b). Putative E2F1-binding sites are indicated by red squares. Quantification of DNA enrichment in the *CDC2* gene promoter was used as a positive control, and *GAPDH* was used as a negative control. Data are presented as the mean  $\pm$  SD of three independent experiments. \*\*,  $p < 0.01$  by Student's *t*-test for unpaired samples to compare differences in enrichment between any specific primer pair and the negative control. (e) Luciferase assays showed the different activities of reporters containing either the wild-type or mutated E2F1-binding sites in KYSE-410 cells, which were released from G0/G1-phase for 8 h. Data are presented as the mean  $\pm$  SD of three independent experiments. \*\*\*,  $p < 0.001$  by Student's *t*-test for unpaired samples to compare differences in relative luciferase activity between reporters with mutant E2F1-binding sites and that with wild-type binding site.

WEE1 protein expression and *miR-424* expression was observed in the NE samples ( $p > 0.05$  by Chi-square test, Supplementary Fig. 6).

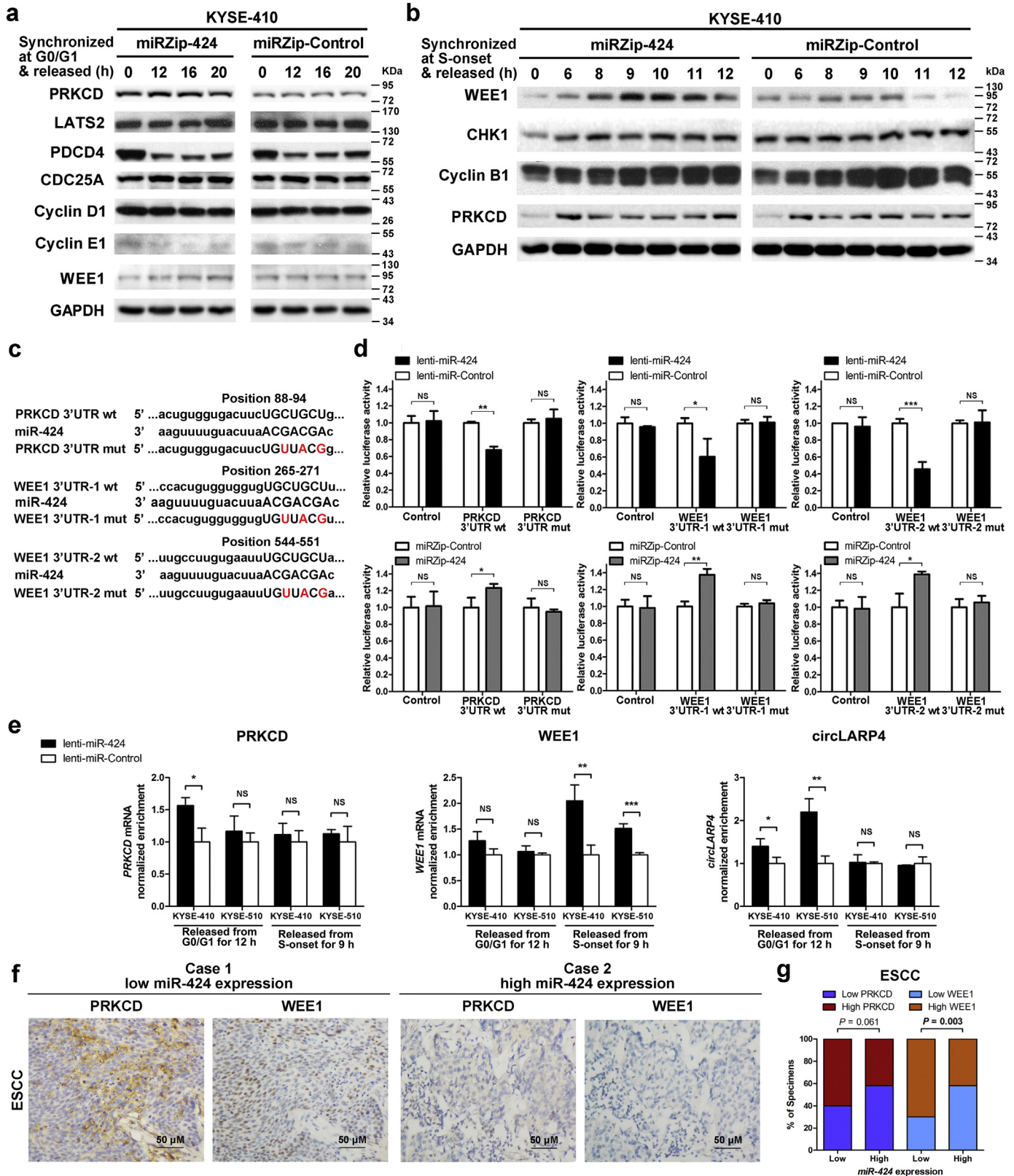
**3.6. *miR-424* modulates cell cycle regulator expression and activity to regulate ESCC cell cycle progression**

The temporal order of cell cycle transition is imposed by the sequential activation or inactivation of CDKs, which is coordinated by interactions with positive regulator cyclins or negative regulator CKIs. Therefore, we examined the active forms and the total protein expression of G1/S and G2/M transition-related cyclins, CDKs, and CKIs in *miR-424*-knockdown and control ESCC cells.

During G1/S transition, western blotting showed that knocking down *miR-424* in KYSE-410 cells increased p21<sup>Cip1</sup> protein expression and decreased p-CDK2 (Thr160) levels, which represent the activated state of CDK2 (Fig. 6a), whereas total CDK2 expression levels remained constant. p21<sup>Cip1</sup> is a member of the CDK-interacting protein/kinase inhibitory protein (CIP/KIP) family that binds to and inhibits the activity of cyclin E-CDK2 complexes and thus functions as a negative regulator of

G1/S progression [37]. However, another member of the CIP/KIP family, p27<sup>Kip1</sup>, did not exhibit expression changes during G1/S transition in *miR-424*-knockdown KYSE-410 cells (Fig. 6a). The negative regulation of p21<sup>Cip1</sup> by *miR-424* did not occur at the transcriptional level, as the mRNA level of p21<sup>Cip1</sup> was not altered by *miR-424* knockdown in KYSE-410 cells (Supplementary Fig. 7). However, knockdown of *miR-424* delayed p21<sup>Cip1</sup> protein degradation when KYSE-410 cells were cultured with cycloheximide to inhibit *de novo* protein synthesis (Fig. 6b), suggesting a possible role of *miR-424* in p21<sup>Cip1</sup> protein stability. It has been reported that p38 MAPK [38] and JNK [39] activation, downstream signaling of PRKCD expression and activation, can enhance the cellular stability of the p21<sup>Cip1</sup> protein without disturbing its mRNA expression [40]. As expected, during G1/S transition, compared with control cells, KYSE-410-*miRZip-424* cells exhibited increased levels of total PRKCD, activated PRKCD (p-PRKCD at Thr505), and downstream activated p38 MAPK (p-p38 MAPK at Thr180/Tyr182) and JNK (p-JNK at Thr183/Tyr185) but not total p38 MAPK and JNK (Fig. 6c).

The mitotic kinase CDC2/Cyclin B is critical for G2/M transition and is maintained in an inactive state until the dephosphorylation of Thr-14



and Tyr-15 at the G2/M border activates CDC2. WEE1 is the kinase responsible for phosphorylating Tyr-15 of CDC2 and hence inhibits CDC2 activity [35]. As shown in Fig. 6d, knockdown of *miR-424* in KYSE-410 cells increased WEE1 expression and CDC2 phosphorylation at Tyr-15 when the cells were at the G2/M border (6 h after release from the onset of S-phase by double-thymidine treatment) compared with control cells.

Collectively, our results showed that knockdown of *miR-424* upregulated PRKCD expression and activated downstream signaling, which further increased p21<sup>Cip1</sup> protein stability to delay G1/S transition in ESCC. On the other hand, the WEE1 upregulation induced by knockdown of *miR-424* maintained the inactivation of CDC2 to postpone G2/M transition in ESCC.

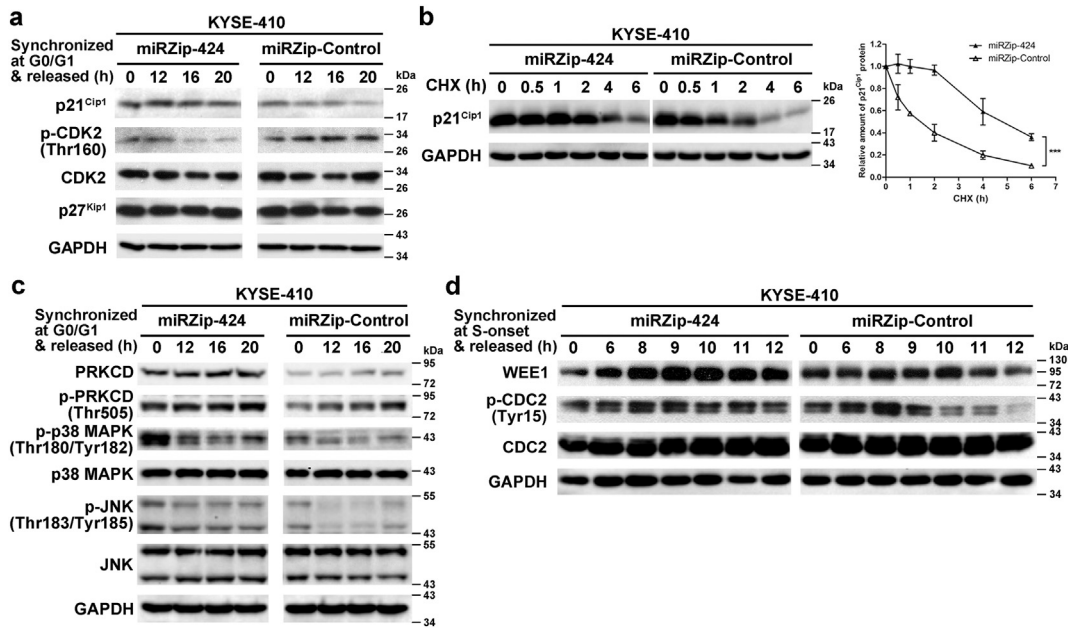


**Fig. 6.** Knockdown of *miR-424* modulates the expression or activity of CDKs or CKIs to regulate ESCC cell cycle progression. (a) Western blotting analysis showed the expression of p21<sup>Cip1</sup>, p-CDK2 (Thr160), and total CDK2 in stable *miR-424*-knockdown or control KYSE-410 cells, which were collected at the indicated time points after release from G0/G1-phase. (b) The stability of the endogenous p21<sup>Cip1</sup> protein in stable *miR-424*-knockdown or control KYSE-410 cells was measured by incubating the cells with 25 μg/ml cycloheximide (CHX). The cells were collected at the indicated time points and analyzed by western blotting (left panel). Quantitation of p21<sup>Cip1</sup> protein levels is shown in the right panel. Data are presented as the mean ± SD of three independent experiments. \*\*\*,  $p < 0.001$  by repeated measures ANOVA. (c) Western blotting analysis showed the expression changes in PRKCD, p-PRKCD (Thr505), p-p38 MAPK (Thr180/Tyr182), p38 MAPK, p-JNK (Thr183/Tyr185), and JNK in stable *miR-424*-knockdown or control KYSE-410 cells, which were collected at the indicated time points after release from G0/G1-phase. (d) Western blotting analysis showed the expression changes in WEE1, p-CDC2 (Tyr15), and CDC2 in stable *miR-424*-knockdown or control KYSE-410 cells, which were collected at the indicated time points after release from the onset of S-phase.

**4. Discussion**

Knowledge about the precise molecular mechanisms that underlie ESCC tumorigenesis is crucial for the development of better diagnostic and therapeutic strategies for ESCC patients. Despite the established roles of a variety of extrinsic and intrinsic signals in regulating ESCC development [6], few studies have identified and validated miRNAs with a role in ESCC [41]. Our study is the first to explore the potential tumor promoter roles and regulatory mechanisms of *miR-424* during cell cycle progression in ESCC.

Previous studies have reported an association between *miR-424* and human cancers. *miR-424* is commonly lost in aggressive breast cancers, and the loss of *miR-424* promotes breast tumorigenesis and chemoresistance by up-regulating two of its targets: *BCL-2* and *IGF1R* [10]. The expression of *miR-424* is lower in cervical cancers than in cervical normal tissues, and enforced expression of *miR-424* inhibits cervical cancer cell growth, migration and invasion via targeting *CHK1* [12]. In hepatocellular carcinoma, *miR-424* inhibits cell proliferation, migration, and invasion by targeting *c-Myb* [13]. *miR-424* directly targets *BCR-ABL* in chronic myeloid cells, and overexpression of *miR-424* suppresses proliferation and induces apoptosis of leukemia cells and sensitizes cells to imatinib treatment [14]. However, *miR-424* has been reported to have elevated expression and a tumor-promoting role in

tongue squamous cell carcinoma [42] and pancreatic cancer [43]. *miR-424* is upregulated in pancreatic cancer and promotes proliferation, migration and invasion while inhibits cell apoptosis in pancreatic cancer cells via targeting *SOCS6* to modulate the ERK1/2 signaling pathway [43]. These discrepancies suggest that the role of *miR-424* is tumor specific and highly dependent on its targets in different types of cancer cells.

In the present study, we first demonstrated that *miR-424* is significantly upregulated in ESCC by microarray analyses, and these results were further validated in paired ESCC and NE tissues. There were some cases in which NE samples exhibited *miR-424* expression levels higher than or close to those in the paired ESCC samples. This is probably due to the phenomenon of field cancerization, in which some morphologically normal cells acquire pro-tumorigenic genetic or epigenetic mutations [44], leading to the increased expression of *miR-424* in NEs. More importantly, *miR-424* expression was identified as an independent predictor of survival in ESCC patients. The poor survival of patients with high *miR-424* expression may be attributable to intrinsic characteristics of the tumor cells that are partly determined by *miR-424*, although no significant correlation was observed between *miR-424* expression and patient clinicopathological characteristics, such as tumor pathological stage or differentiation. Consistent with the clinical data, knockdown of *miR-424* in ESCC cells remarkably suppressed ESCC

**Fig. 5.** *miR-424* targets *PRKCD* and *WEE1* in ESCC cells during G1/S and G2/M transitions, respectively. (a) Stable *miR-424*-knockdown (miRZip-424) and control KYSE-410 cells were synchronized in G0/G1-phase by serum starvation and released for the indicated time points. Western blotting analysis showed the protein expression of potential *miR-424* targets during G1/S transition. (b) Stable *miR-424*-knockdown (miRZip-424) and control KYSE-410 cells were synchronized at the onset of S-phase by double-thymidine block and released for the indicated time points. Western blotting analysis showed the protein expression of potential *miR-424* targets during G2/M transition. (c) The illustration shows the predicted *miR-424* target sequences in the 3'UTRs of the *PRKCD* and *WEE1* mRNAs. (d) Luciferase assays showed different activities of reporters containing the 3'UTRs or mutated 3'UTRs of *PRKCD* and *WEE1* in *miR-424*-overexpressing, *miR-424*-knockdown, and the corresponding control HEK293 cells. Data are presented as the mean ± SD of three independent experiments. \*,  $p < 0.05$ ; \*\*,  $p < 0.01$ ; \*\*\*,  $p < 0.001$ ; or NS, not significant by Student's t-test for unpaired samples. (e) miRNP-IP was performed with an anti-AGO2 antibody on lysates of stable *miR-424*-overexpressing or control KYSE-410 and KYSE-510 cells, and the cells were released from G0/G1 for 12 h or from S-phase onset for 9 h. The quantification of RISC enrichment of *PRKCD*, *WEE1*, and *circLARP4* was determined by qRT-PCR. Data are presented as the mean ± SD of three independent experiments. \*,  $p < 0.05$ ; \*\*,  $p < 0.01$ ; \*\*\*,  $p < 0.001$ ; or NS, not significant by Student's t-test for unpaired samples. (f) Representative immunohistochemical staining images of *PRKCD* and *WEE1* protein in two ESCC cases with low and high *miR-424* expression (Scale bar: 50 μm). (g) The correlation between *miR-424* expression and *PRKCD* or *WEE1* protein expression in 110 ESCC samples was analyzed.  $r = -0.282$ ,  $p = 0.003$  for *WEE1*, and  $r = -0.179$ ,  $p = 0.061$  for *PRKCD* by Chi-square test.

proliferation *in vitro* and tumor formation in a mouse model, while the opposite results were observed after overexpressing *miR-424*. Additionally, overexpression of *miR-424* also promoted the proliferation of the immortalized esophageal epithelial cell line NE1, suggesting that *miR-424* might promote the malignant transformation potential of esophageal normal epithelia cells. Therefore, our findings suggest that *miR-424* functions as a tumor promoter in ESCCs and may be used as a novel prognostic marker for ESCC patients.

After cell synchronization and subsequent flow cytometry analysis, *miR-424* was found to regulate both G1/S and G2/M transitions in ESCC cells. The roles of *miR-424* and its targets in cell cycle progression have been partly explored in previous studies. *miR-424* has been reported to directly target the cell cycle regulators *cyclin E1* [45], *CDC25A* [16], *cyclin D1* [46], and *CHK1* [12] to impair G1/S or G2/M cell cycle transition and inhibit cell proliferation in various kinds of cells. However, expression changes in these previously reported genes were not observed in ESCC cells after knockdown of *miR-424*. When further exploring the underlying mechanisms of *miR-424* in the regulation of ESCC cell proliferation, we found that *miR-424* suppressed the expression of *PRKCD* and *WEE1* by directly targeting their 3'UTRs during G1/S and G2/M transitions, respectively. The correlation of expression between *miR-424* and the *PRKCD* or *WEE1* protein could not be verified in NE samples, suggesting that *PRKCD* or *WEE1* might not be targeted by *miR-424* in NEs. Therefore, the promotion of cell proliferation by *miR-424* overexpression in the immortalized esophageal cell line NE1 might not be mediated by *PRKCD* or *WEE1*. Other previously validated or unidentified *miR-424* targets might be functional in NE tissues. The distinct targets of *miR-424* in ESCC, NE, and other types of cancers explain the tissue specificity of the role of *miR-424* and are consistent with the notion that miRNA-target regulation is context dependent [47,48]. Interestingly, this context-dependent *miR-424* function is not only tissue specific, but also biological process specific. For example, biphasic roles of *miR-424* in ESCC development and progression have been observed. *miR-424* was shown to inhibit ESCC invasion and metastasis by targeting *SMAD7* in a previous study [9] but to promote cell cycle progression by targeting *PRKCD* and *WEE1* in the current study. Similarly, biphasic roles of *miR-424* have also been identified in breast cancer, where *miR-424* facilitates earlier but represses later stage of metastasis [49].

Diverse RNA species, including protein-coding mRNAs and non-coding RNAs, such as long non-coding RNAs, circular RNAs and pseudogenes, can act as natural miRNA sponges. These RNAs communicate with and co-regulate each other by competing specifically for binding to shared miRNAs, thus acting as competing endogenous RNAs (ceRNAs) [50]. In this study, we found that the targeted effects of *miR-424* were cell cycle-phase-specific, as *PRKCD* was targeted during G1/S transition, whereas *WEE1* was targeted during G2/M transition in ESCC cells. During G2/M transition, the gradually accumulating *WEE1* transcript, which has two binding sites for *miR-424*, might bind more *miR-424* by competing with the *PRKCD* transcript. Furthermore, *circLARP4* was proved to bind to *miR-424* in ESCC cells during G1/S transition, especially in KYSE-510 cells, to decrease the binding of *miR-424* to its G1/S target *PRKCD*. It is possible that *PRKCD* and *circLARP4* are ceRNAs during G1/S transition in ESCC cells. However, the reason why *circLARP4* completely abrogated *miR-424* binding to *PRKCD* in KYSE-510 but not KYSE-410 cells is unknown. It has been suggested that ceRNA crosstalk applies mainly to a subset of ceRNAs and miRNAs whose cellular concentrations fall within a specific range of values [50]. The quantitation of the absolute levels of *miR-424* and its target transcript abundance will allow a more precise determination of the effectiveness of ceRNAs.

*PRKCD*, a target of *miR-424* during G1/S transition in ESCCs, is a member of the protein kinase C (PKC) family and can function as a negative regulator of cell cycle progression to inhibit cancer cell proliferation. *PRKCD*-dependent induction of p21<sup>Cip1</sup> is one of the mechanisms by which *PRKCD* inhibits G1/S transition [29]. The control of p21<sup>Cip1</sup>

levels by *PRKCD* appears to be complex, with involvement of both transcriptional [51] and post-transcriptional [40] regulation. In ESCC KYSE-410 cells, *PRKCD* induction by *miR-424* knockdown enhanced p21<sup>Cip1</sup> protein stability by activating downstream p38 MAPK and JAK, which further decreased CDK2 activity to delay G1/S transition. On the other hand, during G2/M transition, *miR-424* targeted *WEE1* in ESCC cells. *WEE1* fulfils a major cell cycle-related function during G2/M transition by directly catalyzing the inhibitory tyrosine 15 phosphorylation of CDC2 and thereby inhibiting the activity of CDC2. Loss of *WEE1* activity would lead to increased CDC2 activity, resulting in a loss of control of cell cycle progression and genome integrity, which would contribute to cancer development [35].

The locus of the human *miR-424* gene is at Xq26.3, which is not commonly amplified or deleted in ESCCs [52]. We also intended to identify the factors involved in the upregulation of *miR-424* in ESCC. Here, we found that expression of *miR-424*, as well as pri-*miR-424* and pre-*miR-424*, increased during G1/S transition. Interestingly, two binding sites of the G1/S transcriptional activator E2F1 were identified in the promoter of *miR-424*. Experiments involving silenced expression of E2F1 in ESCC cell lines demonstrated that E2F1 could regulate pri-*miR-424* expression. In addition, ChIP and luciferase activity assays indicated that E2F1 directly binds to the promoter region of *miR-424* and promotes its transcription and the elevation of *miR-424*. These results suggest a positive feedback loop in which *miR-424* is one of the G1/S genes that are activated by the transcription factor E2F1 and elevation of *miR-424* further increases cyclin-CDK activity and decreases CDK-inhibitory proteins, leading to irreversible cell cycle commitment [27]. In addition to E2F1, HIF1 $\alpha$  has been reported to transcriptionally activate *miR-424* expression under hypoxic conditions, which decreases the sensitivity of colon cancer and melanoma cells to chemotherapy by inhibiting apoptosis [53]. HIF1 $\alpha$  is a widely studied transcription factor that is induced by hypoxia to activate downstream target genes associated with angiogenesis, cell survival, chemotherapy and radiation resistance, invasion, and metastasis of tumors, including ESCCs [54]. Moreover, the transcription factor SMAD4, a downstream factor of the activated TGF $\beta$  pathway, can activate *miR-424* transcription during mammary epithelial involution after pregnancy [26]. TGF $\beta$ /SMAD signaling has been reported to play a role in ESCC invasion and migration. It is possible that *miR-424* expression is regulated transcriptionally by distinct transcription factors during various biological processes, including but not limited to cell proliferation, invasion, and migration.

Mechanistically, our data suggest a model (Fig. 7) in which *miR-424* regulates ESCC cell proliferation. When the cell cycle progresses to mid- or late-G1-phase, the activation of E2F1 induces the transcription of pri-*miR-424*. This primary transcript is processed to generate mature *miR-424*, which in turn regulates the expression of its targets *PRKCD* and *WEE1*, which are components of the cell cycle progression regulation network. *PRKCD* modulates p21<sup>Cip1</sup> protein stability to affect CDK2 activity and G1/S progression, while *WEE1* affects CDC2 activity directly to regulate G2/M progression. Furthermore, *circLARP4* sponges *miR-424* during G1/S transition, which decreases *miR-424* binding to its target *PRKCD* and modulates the effect of *miR-424* on G1/S transition.

Sustained cell proliferation induced by the loss of normal cell cycle control is a hallmark of human cancer [5]. In this study, *miR-424* was found to be upregulated in ESCC and to correlate with poor survival among ESCC patients. The tumor-promoting role of *miR-424* in ESCC was exerted through its regulation of cell cycle progression by directly targeting *PRKCD* and *WEE1* in ESCC cells, which further affected the activity or expression of CDKs or CKIs involved in the G1/S and G2/M cell cycle transitions. *miR-424* may possibly be used as a novel prognostic marker and (or) as an effective therapeutic target for ESCCs. Considering the complexity of miRNA roles, which can be tissue specific and biological process specific, future studies are required to fully elucidate the function of *miR-424* in distinct ESCC cellular behaviors, such as invasion, migration, survival and apoptosis.

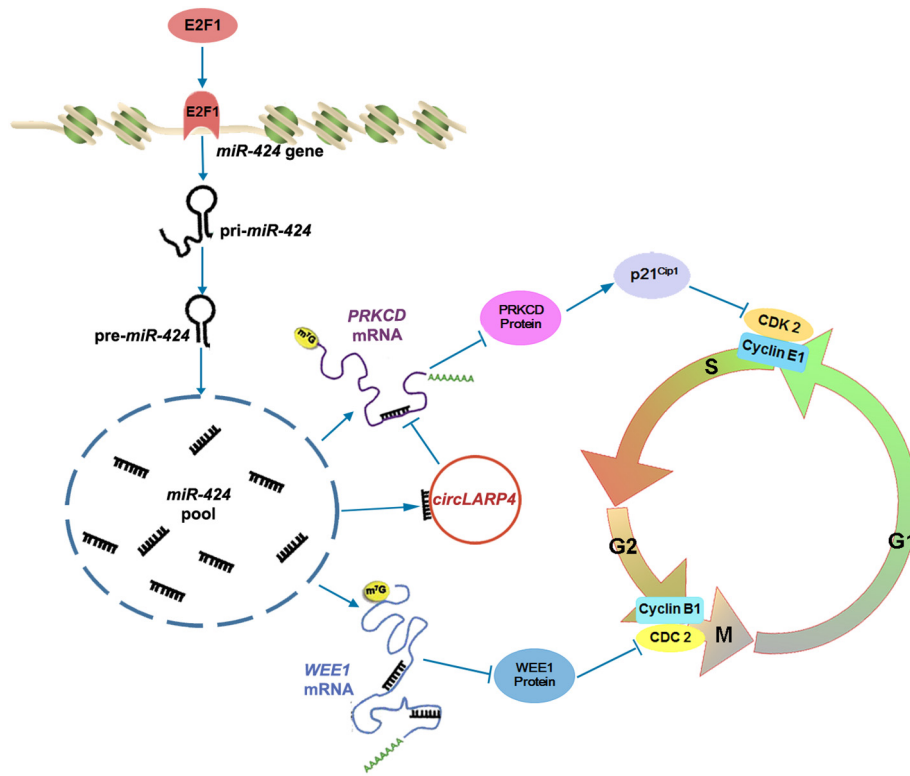


**Fig. 7.** Proposed mechanistic model for the role of *miR-424* in coordinating ESCC cell cycle progression. During G1/S transition, activation of the transcription factor E2F1 induces the expression of the *miR-424* primary transcript. Subsequently, mature *miR-424*, which is generated from *pri-miR-424*, targets *PRKCD* and *WEE1* at the G1/S and G2/M borders, respectively, and these proteins further modulate the expression or activity levels of cell cycle regulators such as p21<sup>Cip1</sup>, CDK2, and CDC2 to regulate ESCC cell cycle progression. However, *circLARP4*, a natural sponge of *miR-424*, can diminish the binding of *miR-424* to *PRKCD* and compromise its regulation of G1/S progression.

**Funding sources**

This work was supported by National Natural Science Foundation of China (Grant Nos 81672356 and 81360365), Guangzhou Science Technology and Innovation Commission (Grant No. 201610010127), Guangdong Talents Special Support Program (Grant No. 201629038), and Guangdong Esophageal Cancer Institute Science and Technology Program (Grant Nos Q201404 and M201701).

**Declaration of interests**

The authors have no financial conflicts to declare.

**Author contributions**

JW, JF, and HY designed the study and wrote the manuscript. JW, YH, and QL performed the experiments and analyzed the data; YL performed the evaluation of IHC staining of tissues; SZ assisted with miRNA microarray data analyses; KL assisted with statistical analysis; XX assisted with the tumor xenograft experiment.

**Appendix A. Supplementary data**

Supplementary data to this article can be found online at <https://doi.org/10.1016/j.ebiom.2018.10.043>.

**References**

[1] Torre LA, Bray F, Siegel RL, Ferlay J, Lortet-Tieulent J, Jemal A. Global cancer statistics, 2012. *CA Cancer J Clin* 2015;65:87–108.  
 [2] Chen W, Zheng R, Baade PD, et al. Cancer statistics in China, 2015. *CA Cancer J Clin* 2016;66:115–32.  
 [3] Dotto GP, Rustgi AK. Squamous cell cancers: A unified perspective on biology and genetics. *Cancer Cell* 2016;29:622–37.

[4] Ingham M, Schwartz GK. Cell-cycle therapeutics come of age. *J Clin Oncol* 2017;35:2949–59.  
 [5] Hanahan D, Weinberg RA. Hallmarks of cancer: The next generation. *Cell* 2011;144:646–74.  
 [6] Ohashi S, Miyamoto S, Kikuchi O, Goto T, Amanuma Y, Muto M. Recent advances from basic and clinical studies of esophageal squamous cell carcinoma. *Gastroenterology* 2015;149:1700–15.  
 [7] Shah MY, Ferrajoli A, Sood AK, Lopez-Berestein G, Calin GA. microRNA therapeutics in cancer - An emerging concept. *EBioMedicine* 2016;12:34–42.  
 [8] David S, Meltzer SJ. MicroRNA involvement in esophageal carcinogenesis. *Curr Opin Pharmacol* 2011;11:612–6.  
 [9] Wang F, Wang J, Yang X, Chen D, Wang L. MiR-424-5p participates in esophageal squamous cell carcinoma invasion and metastasis via SMAD7 pathway mediated EMT. *Diagn Pathol* 2016;11:88.  
 [10] Rodriguez-Barrueco R, Nekritz EA, Bertucci F, et al. miR-424(322)/503 is a breast cancer tumor suppressor whose loss promotes resistance to chemotherapy. *Genes Dev* 2017;31:553–66.  
 [11] Tian Q, Li Y, Wang F, et al. MicroRNA detection in cervical exfoliated cells as a triage for human papillomavirus-positive women. *J Natl Cancer Inst* 2014;106.  
 [12] Xu J, Li Y, Wang F, et al. Suppressed miR-424 expression via upregulation of target gene Chk1 contributes to the progression of cervical cancer. *Oncogene* 2013;32:976–87.  
 [13] Yu L, Ding GF, He C, Sun L, Jiang Y, Zhu L. MicroRNA-424 is down-regulated in hepatocellular carcinoma and suppresses cell migration and invasion through c-Myb. *PLoS One* 2014;9:e91661.  
 [14] Hershkovitz-Rokah O, Modai S, Pasmanik-Chor M, et al. Restoration of miR-424 suppresses BCR-ABL activity and sensitizes CML cells to imatinib treatment. *Cancer Lett* 2015;360:245–56.  
 [15] Liu Q, Fu H, Sun F, et al. miR-16 family induces cell cycle arrest by regulating multiple cell cycle genes. *Nucleic Acids Res* 2008;36:5391–404.  
 [16] Llobet-Navas D, Rodriguez-Barrueco R, de la Iglesia-Vicente J, et al. The microRNA 424/503 cluster reduces CDC25A expression during cell cycle arrest imposed by transforming growth factor beta in mammary epithelial cells. *Mol Cell Biol* 2014;34:4216–31.  
 [17] Wen J, Yang H, Liu MZ, et al. Gene expression analysis of pretreatment biopsies predicts the pathological response of esophageal squamous cell carcinomas to neo-chemoradiotherapy. *Ann Oncol* 2014;25:1769–74.  
 [18] Wen J, Luo K, Liu H, et al. MiRNA expression analysis of pretreatment biopsies predicts the pathological response of esophageal squamous cell carcinomas to neo-adjuvant chemoradiotherapy. *Ann Surg* 2016;263:942–8.  
 [19] Shimada Y, Imamura M, Wagata T, Yamaguchi N, Tobe T. Characterization of 21 newly established esophageal cancer cell lines. *Cancer* 1992;69:277–84.

- [20] Schmittgen TD, Livak KJ. Analyzing real-time PCR data by the comparative C (T) method. *Nat Protoc* 2008;3:1101–8.
- [21] Ji P, Smith SM, Wang Y, et al. Inhibition of gliomagenesis and attenuation of mitotic transition by MIP. *Oncogene* 2010;29:3501–8.
- [22] Fasanaro P, Greco S, Lorenzi M, et al. An integrated approach for experimental target identification of hypoxia-induced miR-210. *J Biol Chem* 2009;284:35134–43.
- [23] Wen J, Luo KJ, Hu Y, Yang H, Fu JH. Metastatic lymph node CHIP expression is a potential prognostic marker for resected esophageal squamous cell carcinoma patients. *Ann Surg Oncol* 2013;20:1668–75.
- [24] Thomson DW, Bracken CP, Goodall GJ. Experimental strategies for microRNA target identification. *Nucleic Acids Res* 2011;39:6845–53.
- [25] Di Leva G, Garofalo M, Croce CM. MicroRNAs in cancer. *Annu Rev Pathol* 2014;9:287–314.
- [26] Llobet-Navas D, Rodriguez-Barrueco R, Castro V, et al. The miR-424(322)/503 cluster orchestrates remodeling of the epithelium in the involuting mammary gland. *Genes Dev* 2014;28:765–82.
- [27] Bertoli C, Skotheim JM, de Bruin RA. Control of cell cycle transcription during G1 and S phases. *Nat Rev Mol Cell Biol* 2013;14:518–28.
- [28] Khan A, Fornes O, Stigliani A, et al. JASPAR 2018: update of the open-access database of transcription factor binding profiles and its web framework. *Nucleic Acids Res* 2018;46 (D260–D6).
- [29] Jackson DN, Foster DA. The enigmatic protein kinase Cdelta: Complex roles in cell proliferation and survival. *FASEB J* 2004;18:627–36.
- [30] Nilsson I, Hoffmann I. Cell cycle regulation by the Cdc25 phosphatase family. *Prog Cell Cycle Res* 2000;4:107–14.
- [31] Dorrello NV, Peschiaroli A, Guardavaccaro D, Colburn NH, Sherman NE, Pagano M. S6K1- and betaTRCP-mediated degradation of PDCD4 promotes protein translation and cell growth. *Science* 2006;314:467–71.
- [32] Li Y, Pei J, Xia H, Ke H, Wang H, Tao W. Lats2, a putative tumor suppressor, inhibits G1/S transition. *Oncogene* 2003;22:4398–405.
- [33] Hydbring P, Malumbres M, Sicinski P. Non-canonical functions of cell cycle cyclins and cyclin-dependent kinases. *Nat Rev Mol Cell Biol* 2016;17:280–92.
- [34] Zhang Y, Hunter T. Roles of Chk1 in cell biology and cancer therapy. *Int J Cancer* 2014;134:1013–23.
- [35] Sorensen CS, Syljuasen RG. Safeguarding genome integrity: the checkpoint kinases ATR, CHK1 and WEE1 restrain CDK activity during normal DNA replication. *Nucleic Acids Res* 2012;40:477–86.
- [36] Zhang J, Liu H, Hou L, et al. Circular RNA\_LARP4 inhibits cell proliferation and invasion of gastric cancer by sponging miR-424-5p and regulating LATS1 expression. *Mol Cancer* 2017;16:151.
- [37] Abukhdeir AM, Park BH. p21 and p27: Roles in carcinogenesis and drug resistance. *Expert Rev Mol Med* 2008;10:e19.
- [38] Blank VC, Bertucci L, Furmento VA, Pena C, Marino VJ, Roguin LP. A chimeric cyclic interferon-alpha2b peptide induces apoptosis by sequential activation of phosphatidylinositol 3-kinase, protein kinase Cdelta and p38 MAP kinase. *Exp Cell Res* 2013;319:1471–81.
- [39] Yokoyama G, Fujii T, Tayama K, Yamana H, Kuwano M, Shirouzu K. PKCdelta and MAPK mediate G(1) arrest induced by PMA in SKBR-3 breast cancer cells. *Biochem Biophys Res Commun* 2005;327:720–6.
- [40] Wakino S, Kintscher U, Liu Z, et al. Peroxisome proliferator-activated receptor gamma ligands inhibit mitogenic induction of p21(Cip1) by modulating the protein kinase Cdelta pathway in vascular smooth muscle cells. *J Biol Chem* 2001;276:47650–7.
- [41] Harada K, Baba Y, Ishimoto T, et al. The role of microRNA in esophageal squamous cell carcinoma. *J Gastroenterol* 2016;51:520–30.
- [42] Boldrup L, Coates PJ, Laurell G, Wilms T, Fahraeus R, Nylander K. Downregulation of miRNA-424: A sign of field cancerisation in clinically normal tongue adjacent to squamous cell carcinoma. *Br J Cancer* 2015;112:1760–5.
- [43] Wu K, Hu G, He X, et al. MicroRNA-424-5p suppresses the expression of SOCS6 in pancreatic cancer. *Pathol Oncol Res* 2013;19:739–48.
- [44] Curtius K, Wright NA, Graham TA. An evolutionary perspective on field cancerization. *Nat Rev Cancer* 2018;18:19–32.
- [45] Nakashima T, Jinnin M, Etoh T, et al. Down-regulation of mir-424 contributes to the abnormal angiogenesis via MEK1 and cyclin E1 in senile hemangioma: its implications to therapy. *PLoS One* 2010;5:e14334.
- [46] Merlet E, Atassi F, Motiani RK, et al. miR-424/322 regulates vascular smooth muscle cell phenotype and neointimal formation in the rat. *Cardiovasc Res* 2013;98:458–68.
- [47] Inui M, Martello G, Piccolo S. MicroRNA control of signal transduction. *Nat Rev Mol Cell Biol* 2010;11:252–63.
- [48] Liu H, Kohane IS. Tissue and process specific microRNA-mRNA co-expression in mammalian development and malignancy. *PLoS One* 2009;4:e5436.
- [49] Drasin DJ, Guarnieri AL, Neelakantan D, et al. TWIST1-induced miR-424 reversibly drives mesenchymal programming while inhibiting tumor initiation. *Cancer Res* 2015;75:1908–21.
- [50] Tay Y, Rinn J, Pandolfi PP. The multilayered complexity of ceRNA crosstalk and competition. *Nature* 2014;505:344–52.
- [51] Saha K, Eckert RL. Methylosome protein 50 and PKCdelta/p38delta protein signaling control keratinocyte proliferation via opposing effects on p21Cip1 gene expression. *J Biol Chem* 2015;290:13521–30.
- [52] Zhang L, Zhou Y, Cheng C, et al. Genomic analyses reveal mutational signatures and frequently altered genes in esophageal squamous cell carcinoma. *Am J Hum Genet* 2015;96:597–611.
- [53] Zhang D, Shi Z, Li M, Mi J. Hypoxia-induced miR-424 decreases tumor sensitivity to chemotherapy by inhibiting apoptosis. *Cell Death Dis* 2014;5:e1301.
- [54] Semenza GL. Defining the role of hypoxia-inducible factor 1 in cancer biology and therapeutics. *Oncogene* 2010;29:625–34.